Diploma Thesis

Synthesis and Reactivity of novel Molybdenum and Tungsten PNP Pincer Complexes

accomplished at the

Institute for Applied Synthetic Chemistry
Department of Chemistry
Technical University of Vienna

under the supervision of

Ao.Univ.Prof. DI Dr.techn. Karl Kirchner

and the tutorship of

DI Dr.techn. Eva Becker

by

Robert Lichtenberger

Schallergasse 34/1-3
1120 Wien

Vienna, October 2006

Abstract

This work describes the synthesis of novel molybdenum and tungsten PNP pincer complexes based on a new class of PNP ligands containing amino bridges between the aromatic backbone and the neutral phosphorus donors. The ligands have been prepared by simple condensation reactions between 2,6-diaminopyridine and chlorophosphines or -phosphites in toluene using Et_3N and/or *n*-BuLi as base to give the PNP pincer ligands PNP-^{i}Pr, PNP-^{t}Bu, PNP-BIPOL, and PNP-TAR^{Me}.

These ligands were reacted with $M(CO)_6$ (M = Mo, W) in CH_3CN to give pincer complexes of the types Mo(PNP-^{i}Pr)$(CO)_3$, Mo(PNP-^{t}Bu)$(CO)_3$, and W(PNP-^{i}Pr)$(CO)_3$ via intermediates $M(CO)_3(NCCH_3)_3$. $Mo(CO)_4(NCCH_3)_2$ was prepared from $Mo(CO)_6$ by reduction of the reaction temperature and time. Addition of the ligands PNP-^{i}Pr and PNP-^{t}Bu to a solution of $Mo(CO)_4(NCCH_3)_2$ resulted in the formation of the complexes Mo(PN(P)-^{i}Pr)$(CO)_4$ and Mo(PN(P)-^{t}Bu)$(CO)_4$ where the PNP ligand is coordinated in a bidentate fashion via the pyridine nitrogen and one of the phosphorus atoms.

Starting from the carbonyl pincer complex Mo(PNP-^{i}Pr)$(CO)_3$ the reactivity of the molybdenum complexes was studied by reacting it with halogens to study its ability to undergo oxidative addition reactions. The reaction proceeded well with iodine and bromine and resulted in seven-coordinated halocarbonyl PNP pincer complexes of the type $[Mo(PNP)(CO)_3X]X$ (X = I, Br). It was shown that this complex could be prepared also via an alternative synthetic route starting from $MoI_2(CO)_3(NCCH_3)_2$ and PNP-^{i}Pr. If the reaction was carried out in CH_3CN one CO ligand was replaced by this solvent and $[Mo(PNP\text{-}^{i}Pr)(CO)_2(NCCH_3)I]I$ was obtained.

Preliminary studies also showed that is was possible to form a hydride species by treatment of Mo(PNP-^{i}Pr)$(CO)_3$ with CF_3COOH as hydride donor.

$[Mo(PNP\text{-}^{i}Pr)(CO)_2(NCCH_3)I]I$ was reduced in the presence of zinc to obtain the complex $Mo(PNP\text{-}^{i}Pr)(CO)_2(NCCH_3)$. The reactivity of these complexes towards alkynes was studied with the objective to prepare vinylidene complexes. Unfortunately, all attempts to obtain such species were unsuccessful.

Acknowledgements

First I would like to thank Prof. Karl Kirchner, who introduced me into organometallic chemistry, for providing this interesting theme for me and for his support during the whole work.

Prof. Kurt Mereiter I acknowledge for the measurement of the crystal structure.

Eva Becker and Sonja Pavlik I thank for their restless support and help during my work in this research group, for always having an ear for my problems and for lots of interesting discussions.

Julia Wiedermann, David Benito-Garagorri and Vladica Bocokić I thank for their support during my work with them. Furthermore I would like to thank them for their friendship and for the most pleasant atmosphere within the "Pincer Crew". Thanks also to Martin Pollak and Robert Potzmann. You all together turned the last months from hard work to "Urlaub bei Freunden".

All colleges from the "class of 01" I would like to thank for making my study to one of the most exciting times of my life. Special thanks to Christian Heller, who went with me through countless examinations and experiences and became a really dear friend.

Thanks to all my friends outside the university, who always reminded me of the pleasures beside chemistry and enriched my life. Special thanks to my dear old friends from Linz, who never forgot me and made every stay at home to a unique experience.

Special thanks to my parents to make my study possible by their support in all fields and for their endless love. Thanks also to my brother Peter, for being the best big brother I know. You all are my biggest icons.

Thanks to Kolja for being the hairiest friend I've ever had and for pressing all the keys he shouldn't.

Finally I want to dedicate this work to the most special and important person in my life: my wife Alexandra. Without you, all the work of the last years would not have been possible. Thanks for your restless love and for making my life what it is: perfect.

“…und da sind wir auch schon wieder mit der ganzen Geschichte durch.”

(Walter Steiner)

Contents

1 Introduction and Scope 1

2 General Considerations 4

2.1 Pincer Ligands 4

2.2 Transition Metal Pincer Complexes 5

2.3 Molybdenum and Tungsten Complexes 8

3 Results and Discussion 11

3.1 Preparation of the Ligand Building Blocks 11

3.2 Preparation of the Ligands 12

3.3 Preparation of the Molybdenum and Tungsten Precursors 16

3.3.1 Preparation of the Tricarbonyltris(acetonitrile) and Tetracarbonylbis(acetonitrile) Precursors 16

3.3.2 $MoI_2(CO)_3(NCCH_3)_2$ 18

3.3.3 $Mo(\eta^3\text{-allyl})(CO)_2(NCCH_3)_2Br$ 19

3.4 Preparation of the Pincer Complexes 19

3.4.1 Tricarbonyl Complexes 19

3.4.2 Tetracarbonyl Complexes 22

3.5 Reactions of the Pincer Complexes 24

3.5.1 Reactions with Halogens 24

3.5.2 Reaction with Methyl Iodide 28

3.5.3 Reaction with CF_3COOH 29

3.5.4 Reaction with Allyl bromide 30

3.6 Reactions of $[Mo(PNP\text{-}^iPr)(CO)_2(NCCH_3)I]I$ 31

3.6.1 Reaction with Methyl Iodide 31

3.6.2 Reduction to $Mo(PNP\text{-}^iPr)(CO)_2(NCCH_3)$ 31

3.7 Self-Exchange Atom Transfer Experiments 32

3.8 Reaction with Alkynes 33

4 Summary and Outlook 35

5 Experimental Section 37

5.1 General 37

5.2 Preparation of the Ligand Building Blocks 38

5.2.1 Preparation of 2-Chlorodibenzo[*d*,*f*]-1,3,2-dioxaphosphepine (BIPOL-PCl) (**1a**) 38

5.2.2 Preparation of 2-Chloro-(4*R*,5*R*)-dicarbomethoxy-1,3,2-dioxaphospholane (TAR^{Me}-PCl) (**1b**) 39

5.3 Preparation of the Ligands....40
5.3.1 Preparation of *N,N'*-Bis(diisopropylphosphino)-2,6-diaminopyridine (PNP-^{i}Pr) (**2a**)...40
5.3.2 Preparation of *N,N'*-Bis(di-*tert*-butylphosphino)-2,6-diaminopyridine (PNP-^{t}Bu) (**2b**) 41
5.3.3 Preparation of *N,N'*-Bis(dibenzo[*d,f*]-1,3,2-dioxaphosphepine)-2,6-diaminopyridine (PNP-BIPOL) (**2c**) 42
5.3.4 Preparation of *N,N*'-Bis((4*R*,5*R*)-dicarbomethoxy-1,3,2-dioxaphospholane)-2,6-diaminopyridine (PNP-TAR^{Me}) (**2d**) 43
5.4 Preparation of the Molybdenum and Tungsten Precursors 44
5.4.1 Preparation of $Mo(CO)_3(NCCH_3)_3$ (**3a**)....44
5.4.2 Preparation of $Mo(CO)_4(NCCH_3)_2$ (**3b**) 44
5.4.3 Preparation of $W(CO)_3(NCCH_3)_3$ (**3a'**) 45
5.4.4 Preparation of $MoI_2(CO)_3(NCCH_3)_2$ (**4**) 45
5.4.5 Preparation of Mo(η^3-allyl)$(CO)_2(NCCH_3)_2$Br (**5**) 46
5.5 Preparation of the Pincer Complexes....47
5.5.1 Preparation of Mo(PNP-^{i}Pr)$(CO)_3$ (**6a**) 47
5.5.2 Preparation of Mo(PNP-^{t}Bu)$(CO)_3$ (**6b**) 48
5.5.3 Preparation of W(PNP-^{i}Pr)$(CO)_3$ (**6a'**)....49
5.5.4 Preparation of Mo(PN(P)-^{i}Pr)$(CO)_4$ (**7a**)....50
5.5.5 Preparation of Mo(PN(P)-^{t}Bu)$(CO)_4$ (**7b**) 51
5.6 Reactions of the Complexes....52
5.6.1 Reaction with Halogens....52
5.6.2 Preparation of Mo(PNP-^{i}Pr)$(CO)_2(NCCH_3)$ (**11**) 56
5.6.3 Reaction of Mo(PNP-^{i}Pr)$(CO)_3$ (**6a**) with CF_3COOH 57
5.6.4 Self-Exchange Atom Transfer Experiment....57
5.7 Crystallographic data 58

List of Figures

Figure 1.1 Schematic structure of pincer complexes 1
Figure 1.2 Modular system of amino-bridged PNP pincer ligands 2
Figure 1.3 Comparison of the meridional arrangement 3
Figure 2.1 Schematic structure of pincer ligands 4
Figure 2.2 Examples of different types of pincer ligands 5
Figure 2.3 Binding modes of NCN pincer complexes 6
Figure 2.4 Typical coordination geometries of pincer complexes 6
Figure 2.5 Synthetic routes to PCP pincer complexes 7
Figure 2.6 Examples for achiral (left) and chiral (right) Schrock catalysts 9
Figure 2.7 Example of an epoxidation catalyst 9
Figure 2.8 The four main geometries of seven-coordinated complexes 10
Figure 3.1 Preparation of the Chlorophosphites (1a and 1b) 11
Figure 3.2 Comparison of the synthetic routes to alkyl- and amino-bridged PNP ligands 12
Figure 3.3 Tautomerism between 1,3-dihydroxypyridine and 6-hydroxypyridin-2-one 13
Figure 3.4 Triazine-based and N-alkylated amino-bridged PNP pincer ligands 14
Figure 3.5 Preparation of the PNP ligands (2a-d) 14
Figure 3.6 Preparation of $M(CO)_3(NCCH_3)_3$ (M = Mo, W) (3a and 3a') 17
Figure 3.7 Preparation of *mer*-$Mo(CO)_3(NCCH_3)_3$ (3a) and *cis*-$Mo(CO)_4(NCCH_3)_2$ (3b) 18
Figure 3.8 Preparation of $MoI_2(CO)_2(NCCH_3)_2$ (4) 18
Figure 3.9 Preparation of Mo(η^3-allyl)$(CO)_2(NCCH_3)_2Br$ (3) 19
Figure 3.10 Preparation of the tricarbonyl pincer complexes (6a, 6a', and 6b) 20
Figure 3.11 Preparation of the tetracarbonyl pincer complexes (7a and 7b) 22
Figure 3.12 Reaction of Mo(PNP-^{i}Pr)$(CO)_3$ (6a) with halogens 24
Figure 3.13 Two synthetic routes to [Mo(PNP-^{i}Pr)$(CO)_3$I]I (8a) 25
Figure 3.14 Structural view of [Mo(PNP-^{i}Pr)$(CO)_3$Br]Br (9a) showing 20 % thermal ellipsoids 27
Figure 3.15 Alternative structural view of 9a showing 20 % thermal ellipsoids (C-bound H atoms and Br^- omitted for clarity) 28
Figure 3.16 Reaction of K[MoTp$(CO)_3$] with methyl iodide 29
Figure 3.17 Reaction of K[MoTp$(CO)_3$] with acetic acid 29
Figure 3.18 Reaction of K[MoTp$(CO)_3$] with allyl bromide 30
Figure 3.19 Reactions with allyl bromide 30
Figure 3.20 Preparation of Mo(PNP-iPr)$(CO)_2(NCCH_3)$ (11) 32
Figure 3.21 Self-exchange atom transfer experiment 33
Figure 3.22 Synthesis of a tungsten vinylidene complex 34
Figure 3.23 Used alkynes 34

List of Tables

Table 3.1 Selected ^{1}H and $^{31}P\{^1H\}$ NMR resonances of the PNP ligands 15
Table 3.2 Selected ^{1}H and $^{31}P\{^1H\}$ NMR resonances of the tricarbonyl PNP pincer complexes 20
Table 3.3 Comparison of selected ^{1}H and $^{31}P\{^1H\}$ NMR resonances of the PNP ligands and their molybdenum tricarbonyl complexes 21
Table 3.4 Comparison between the $^{31}P\{^1H\}$ NMR resonances of the tricarbonyl complexes, tetracarbonyl complexes, and free ligands 23
Table 3.5 Comparison of selected ^{1}H and $^{31}P\{^1H\}$ NMR resonances of the halide complexes 25
Table 5.1 Crystal data and structure refinement for [Mo(PNP-^{i}Pr)$(CO)_3$Br]Br 58
Table 5.2 Bond lengths for [Mo(PNP-^{i}Pr)$(CO)_3$Br]Br 59
Table 5.3 Hydrogen bonds in Mo(PNP-^{i}Pr)$(CO)_3$ 59

List of Abbreviations

NMR	Nuclear Magnetic Resonance
ppm	parts per million
equiv.	equivalent
r.t.	room temperature
^{i}Pr	isopropyl
^{t}Bu	*tert*-butyl
Ph	phenyl
Et	ethyl
acac	acetylacetonate
n-Bu	*n*-Butyl
Cp	cyclopentadienyl
Tp	trispyrazolylborat
Mes	mesityl
Cy	cyclohexyl
AcOH	acetic acid
Et_3N	triethylamine
NBS	*N*-bromosuccinimide
NMP	*N*-methylpyrrolidone
DMA	*N*,*N*-dimethyl acetamide

1 Introduction and Scope

Since the first pincer type ligands were synthesized in the late 1970s[1,2], they continuously gained more interest and attention in organometallic and organic chemistry. As shown in Figure 1.1 the name "pincer" derives from the tridentate binding mode to metal centers, which reminds one of a pincer fixing the metal atom.

Usually pincer complexes consist of a planar tridentate ligand bound to a metal center via two 2-electron-donors, and a carbon-metal σ-bond, respectively. The ligands base on an aromatic backbone of 1,3-disubstituted benzenes.

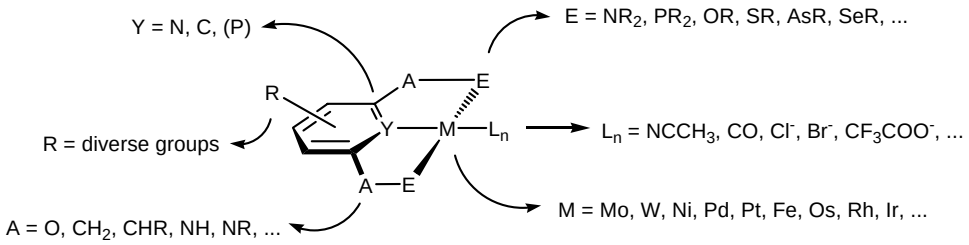

Figure 1.1 Schematic structure of pincer complexes

Due to the large number of modifications of the aromatic system (R, Y), the spacers (A), and the donor atoms (E) as well as the central metal atom (M), a modular system for the preparation of various organometallic compounds arises. In this way compounds could be designed for a wide range of applications through variation of the chemical, electronic, steric, and stereochemical properties of the complexes. Pincer ligands and their complexes with various transition metals have become useful tools in the hands of preparative chemists, especially as catalysts for diverse chemical reactions[3].

Most of the published work dealing with pincer ligands and their complexes concentrates on anionic PCP pincer complexes based on 1,3-disubstituted benzenes. But also analogous PNP pincer complexes featuring a 2,6-disubstituted pyridine backbone have been reported and are meanwhile widely used in transition metal chemistry. In contrast to the anionic PCP pincer ligands, PNP pincer ligands coordinate via three neutral 2-electron-donors. Therefore, for the complexation no C–H activation is necessary and the formation of the pincer complexes proceeds under milder conditions.

---

[1] Moulton, C. J.; Shaw, B. L. *J. C. S. Dalton* **1976**, 1020.
[2] van Koten, G.; Timer; K., Noltes, J. G.; Spek, A. L. *J. Chem. Soc. Chem. Commun.* **1978**, 250.
[3] Singleton, J T. *Tetrahedron* **2003**, *59*, 1837.

Haupt and coworkers developed a new and easy approach to a modular system of amino bridged PNP pincer ligands and complexes based on 2,6-diaminopyridine[4]. In this group this basic idea was further advanced to obtain a comprehensive system of building blocks which allows the modular design of various new PNP[5] and PCP[6] pincer complexes. This method is not only limited to chlorophosphines but also chlorophosphites could be used. The use of chlorophosphites starting from chiral diols gives way to the introduction of chirality to pincer complexes.

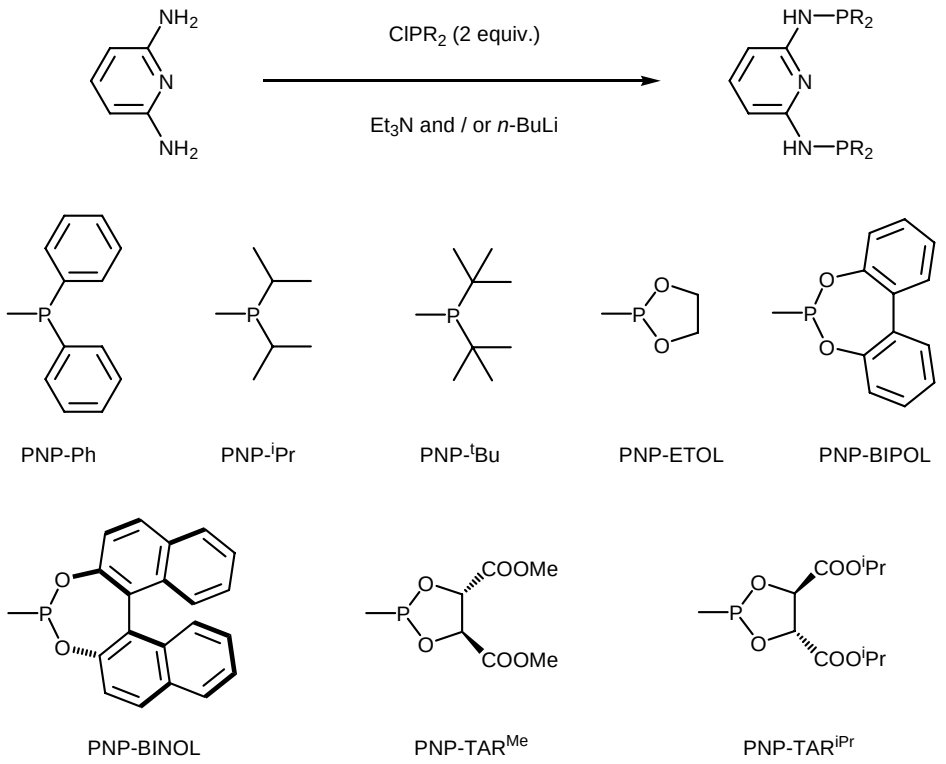

Figure 1.2 Modular system of amino-bridged PNP pincer ligands

The first part of this work is dedicated to the synthesis of various PNP pincer ligands as starting materials for new molybdenum and tungsten PNP pincer complexes including alkyl substituted PNP pincer ligands and ligands based on phosphites.

In contrast to metals like Pd or Pt, examples for PNP pincer complexes of group 6 transition metals are comparatively rare. To our knowledge there are only the complexes M(PNP-Ph)$(CO)_3$ (M = Cr, Mo, W) of Haupt and coworkers and the dinuclear molybdenum complex [Mo(PNP)Mo(HPCy_2)Cl_3]

[4] (a) Schirmer, W.; Flörke, U.; Haupt, H.-J. *Z. anorg. Allg. Chem.*, **1987**, *545*, 83. (b) Schirmer, W.; Flörke, U.; Haupt, H.-J. *Z. anorg. Allg. Chem.*, **1989**, *574*, 239.
[5] Benito-Garagorri, D.; Becker, E.; Wiedermann, J.; Lackner, W.; Pollak, M.; Mereiter, K.; Kisala, J.; Kirchner, K. *Organometallics* **2006**, *25*, 1900.
[6] Benito-Garragori, D.; Bocokić, V.; Mereiter K.; Kirchner, K. *Organometallics*, **2006**, *25*, 3817.

(PNP = 2,6-bis-(dicyclohexylphosphinomethyl)pyridine) recently published by Walton and coworkers[7].

The second part of this work focuses on the preparation of PNP pincer complexes. The use of alkyl substituted phosphines instead of the aryl substituted led to the new complexes M(PNP-^{i}Pr)(CO)$_3$ (M = Mo, W) and Mo(PNP-^{t}Bu)(CO)$_3$ with a similar coordination geometry but different electronic and steric properties. This opened access to a new class of molybdenum complexes with three carbonyl ligands in a meridional arrangement. Nearly all other molybdenum carbonyl complexes show a facial arrangement of the carbonyl ligands, e.g., complexes with Cp[8] or Tp[9] ligands (see Figure 1.3).

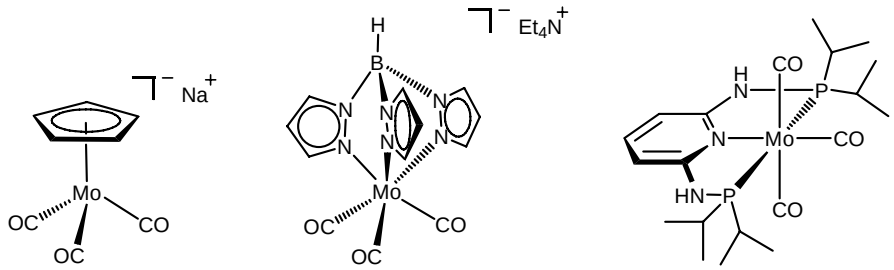

Figure 1.3 Comparison of the meridional arrangement

The final part of this work deals with the reactivity of the complexes. Key reactions like oxidative addition or ligand exchange should be studied by treatment of the new complexes with I_2 and Br_2 under different reaction conditions. Products of these reactions should be characterized by NMR spectroscopy and X-ray crystallography.

[7] Lang, H.-F.; Fanwick, P. E.; Walton, R. A. *Inorg. Chim. Acta* **2002**, *329*, 1.
[8] (a) Doney, J. J.; Bergman, R. J.; Heathcock, C. H. *J. Am. Chem. Soc.* **1985**, *107*, 3724. (b) Hughes, R. P.; Klaeui, W.; Reisch, J. W.; Mueller, A. *Organometallics* **1985**, *4*, 1761.
[9] (a) Trofimenko, S. *J. Am. Chem. Soc.* **1967**, *89*, 3904. (b) Trofimenko, S. *J. Am. Chem. Soc.*, **1969**, *91*, 588. (c) Enemark, J. H.; Marabella, P. *J. Organomet. Chem.* **1982**, *226*, 57. (d) Shiu, K.-B.; Lee, J. Y.; Wang, Y.; Cheng, M.-C.; Wang, S.-L.; Liao, F.-L. *J. Organomet. Chem.* **1993**, *453*, 211.

2 General Considerations

2.1 Pincer Ligands

Pincer ligands are ternary coordinating ligands, also called tridentate ligands (see Figure 2.1). The concept of this type of ligands was developed by Shaw and coworkers in the 1970s. This early work deals with 1,3-disubstituted benzene derivatives featuring $–CH_2–$ spacers and neutral 2-electron-donors. The binding to the metal fragment results from a carbon-metal σ-bond of the benzene ring and two neutral two electron donors E, which were phosphine or amine fragments in the first complexes. Accordingly, these ECE pincer ligands are called PCP and PNP ligands, respectively, indicating the atoms coordinated to the metal center (see Figure 2.1).

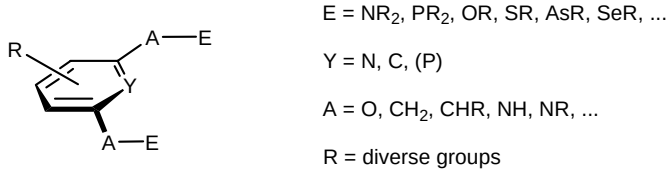

Figure 2.1 Schematic structure of pincer ligands

Later the concept of pincer type ligands has been widened to non aromatic systems and to hetero aromatic systems, in particular based on pyridine. Pincer ligands with a pyridine backbone are of particular interest for this work. In contrast to benzene based systems, pyridine based systems are neutral. Both ligand types have been reported with neutral 2-electron donor systems like $–NR_2$, $–PR_2$, –SeR, –OR, or –SR as well as systems with two different donor atoms[10,11]. Thus there is a wide variety of PCP, NCN, PNP, CNC, PCN and other pincer ligands and complexes[10,12]. Other ways of modifying the properties of pincer ligands are substitution of the backbone or the spacer atoms A. Some examples for different types of pincer ligands are given in Figure 2.2[2,5,10].

---

[10] (a) Castonguay, A.; Sui-Seng, C.; Zaragarina, D.; Beauchamp, A. L. *Organometallics* **2006**, *25*, 602. (b) Danopoulos, A. A.; Tulloch, A. A. D.; Winston, S.; Eastham, G.; Hursthouse, M. B. *Dalton Trans.* **2003**, 1009. (c) Churruca, F.; SanMartin, R.; Tellitu, I.; Domínguez, E. *Tetrahedron Lett.*, **2006**, *47*, 3233.

[11] (a) Peveling, K.; Henn, M.; Loew, C.; Mehring, M.; Schuermann, M.; Costisella, B.; Jurkschat, K. *Organometallics* **2004**, *23*, 1501. (b) Yao, Q.; Sheets, M. *J. Org. Chem.* **2006**, *71*, 5384. (c) van Manen, H.-J.; Nakashima, K.; Shinkai, S.; Kooijman, H.; Spek, A. L.; van Veggel, F. C. J. M.; Reinhoudt, D. N. *Eur. J. Inorg. Chem.* **2000**, 2533.

[12] Poverenov, E.; Gandelman, M.; Shimon, L. J. W.; Rozenberg, H.; Ben-David, Y.; Milstein, D. *Chem. Eur. J.* **2004**, *10*, 4673.

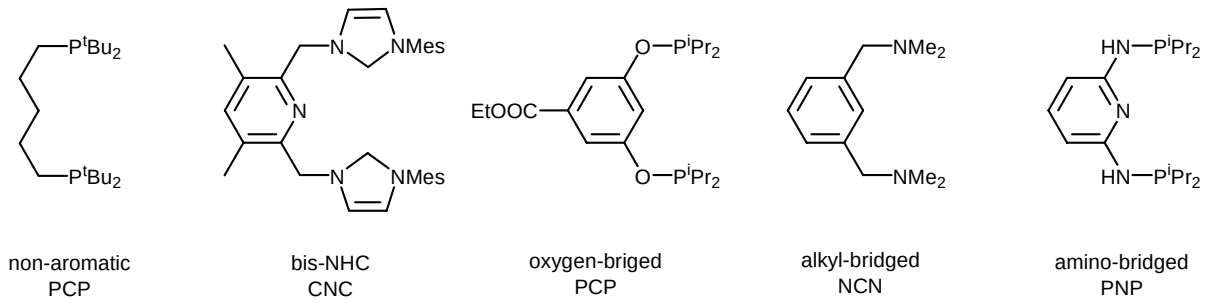

Figure 2.2 Examples of different types of pincer ligands

Phosphines are of immanent importance in organometallic chemistry because of the wide variability of their properties. Beside the steric properties also the electronic behavior like the donor/acceptor-properties can be modified via the use of different substituents. Phosphines are σ-donor / π-acceptor ligands, which donate electron density from their lone-pair into an empty d-orbital of the metal center and simultaneously interact with filled d-orbitals of the metal center via their empty σ*-orbitals. This binding mode is similar to that of carbonyl-ligands, which allow π-backbonding to their π*-orbitals.

Another advantage of phosphine ligands is their detectability via ^{31}P NMR spectroscopy. The NMR active isotope ^{31}P is a spin-½-nucleus and because of its 100% natural occurrence this method is highly sensitive, despite the fact that the sensitivity of the nucleus is only 6.6 % of ^{1}H. Coordination to a metal center normally deshields the phosphorus and in combination with the coupling to ^{1}H and ^{13}C nuclei NMR spectroscopy is a powerful instrument for the characterization of PNP pincer complexes.

2.2 Transition Metal Pincer Complexes

As mentioned earlier, pincer ligands are tridentate ligands, and in most cases they are ternary coordinated to the metal center. For NCN pincer complexes examples of different binding modes have been observed, reaching from κ^1-C over κ^2-N,C to κ^3-N,C,N[13]. If those NCN ligands are coordinating in a ternary mode, they mostly adapt meridional geometry. Only in very few cases they form a facial geometry. Examples for the different binding modes in different NCN pincer complexes are given in Figure 2.3.

[13] Albrecht, M.; van Koten, G. *Angew. Chem. Int. Ed.* **2001**, *40*, 3750.

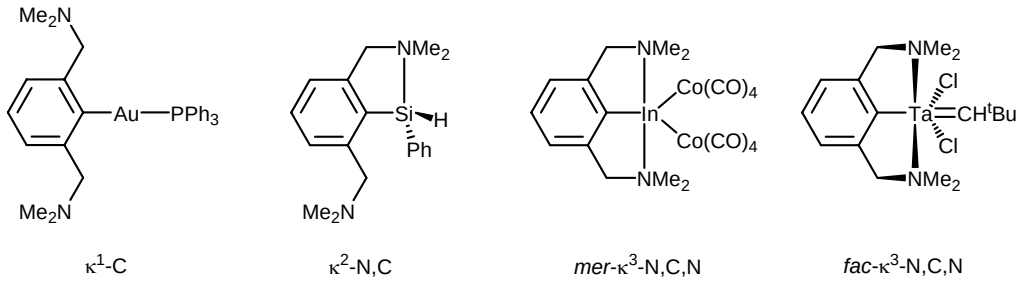

Figure 2.3 Binding modes of NCN pincer complexes

Binding modes deviating from meridional arrangement haven not been observed for other classes of pincer complexes like SCS-, PCP- or PNP pincer ligands. For this ligands the *mer*-κ^3-P,N,P structure is the dominant one, and sometimes ligands which do not bind in this mode are not called pincer ligands. In the meridional geometry the two phosphorus atoms are in trans-position and the aromatic system is forced into a conformation which is coplanar to the plane spanned by the pyridine-N, the metal center and the phosphorus atoms, which could be seen as members of two 5-membered metallacycles. So the ligand– except the substituents at the phosphorus – forms a plane which is coplanar to the d^8-square-planar coordination geometry or to the basal plane of the square pyramids of a d^6-octahedral coordination sphere (see Figure 2.4).

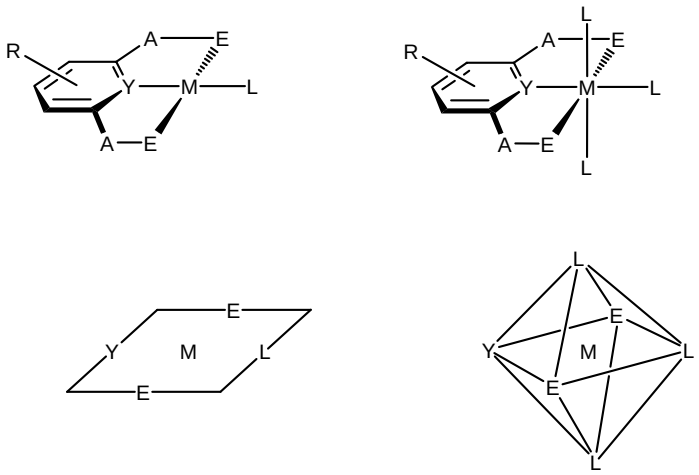

Figure 2.4 Typical coordination geometries of pincer complexes

There are different pathways for the complex formation with neutral and anionic pincer ligands. The complexation of anionic ECE pincer ligands requires the cleavage of a C–R_1 bond (R_1 = H, CH_3, SiR_3, Li, Cl, Br, I, …).

Methods for the complexation of benzene based ligands are direct metallation, oxidative addition, transmetallation, and transcyclometallation (see Figure 2.5).

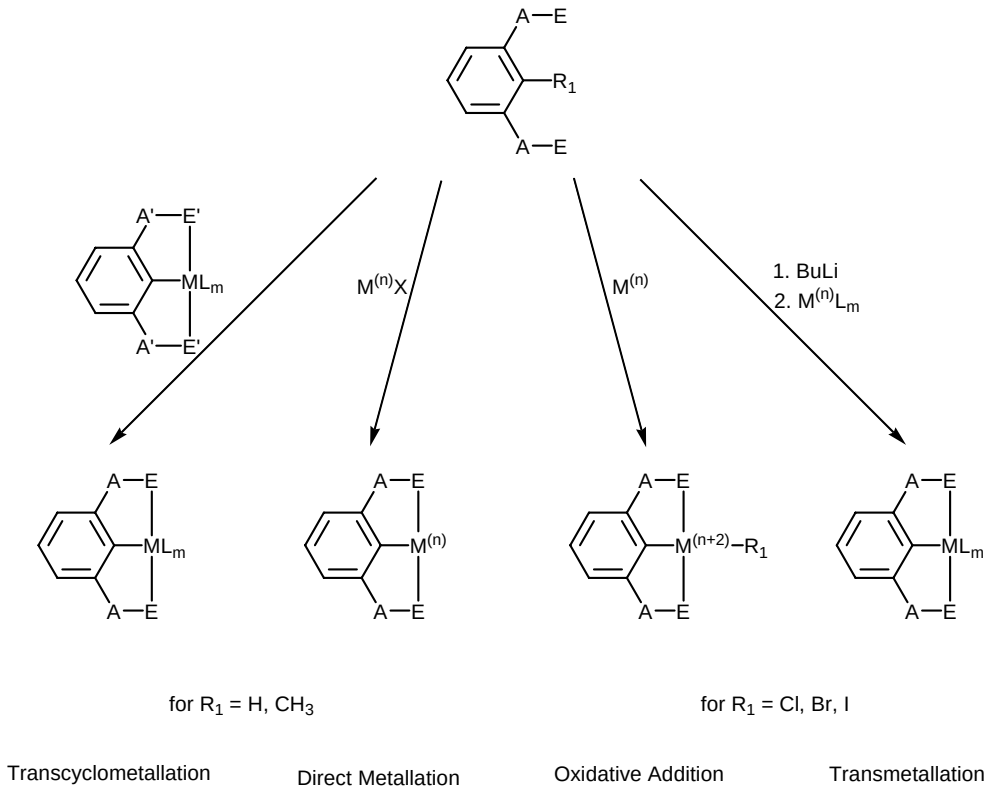

Figure 2.5 Synthetic routes to PCP pincer complexes

In the case of the direct metallation the C–R_1 bond of the ligand is activated and broken by a metal precursor. These metal precursors are often metal halides or complexes with labile ligands like acetonitrile- or aquo-complexes. If R_1 = H and a metal halide is used, an acid is formed as byproduct, which can be a problem for acid sensitive ligands. The first PCP pincer complexes were synthesized via this method, but for NCN-ligands the method implies some problems[14]. It is assumed that previous to the bond activation the metal has to be coordinated via the two neutral electron donors. As the N–M bond is weaker than other coordinative bonds like P–M or S–M, the metallation of NCN pincer ligands leads to other (kinetically controlled) products.

If an oxidative addition step is used for the complexation, metal centers in low oxidation states are necessary, because during the reaction the oxidation state switches from M^n to M^{n+2}. The main advantage of this method is that no acid HX is formed and the oxidative addition proceeds under mild reaction conditions[15,16].

[14] Steenwinkel, P.; Gossage, R. A.; van Koten, G. *Chem. Eur. J.* **1998**, *4*, 759.
[15] Myazaki, F.; Yamaguchi, K.; Shibasaki, M. *Tetrahedron Lett.* **1999**, *40*, 7379.

For the transmetallation, an organometallic species has to be prepared reacting the pincer ligands with a reactive metal, mostly Li. These species in turn reacts with the transition metal salt to give the desired pincer complex.

In the transcyclometallation a transition metal pincer complex is reacted with another, more reactive, pincer ligand. This means that the neutral donors E of the free pincer ligand have to be bound stronger to the metal than those of the precursor complex E' (see Figure 2.5). This worked well for E = $–PPh_3$ or –SEt and E' = $–NMe_2$. This method for the preparation of pincer complexes is quite new and is still under development.

The preparation of pyridine based complexes works under milder conditions via a simple ligand exchange mechanism, because no bond activation or cleavage is needed. Pincer complexes of the PNP type have been synthesized with a wide variety of transition metals, e.g. with Fe, Ru, Rh, Ir, Pd, and Pt[17].

Pincer transition metal complexes are widely used in catalytic and stoichiometric reactions. Examples are the use in the Heck cross-coupling reaction[18,19] or the Suzuki-Miyaura cross-coupling reaction[20,21], to name just a few.

2.3 Molybdenum and Tungsten Complexes

Molybdenum compounds are found to be stable in a wide variety of oxidation states (Mo^0 – Mo^{IV}) and because of the possibility to switch easily between those oxidation states they are used in catalytic applications.

The Schrock catalysts are among the most active catalysts known for olefin metathesis[22]. The catalysts all base on the same components: a Mo^{IV} metal center, an alkylidene ligand, an imidoalkyl ligand and two single or one chelating alkoxide ligand(s). By using chiral alkoxides stereochemical information is introduced and enantioselective catalysis is possible.

---

[16] Van de Kuil, L. A.; Luitjes, H.; Grove, D. M.; Zwikker, J. W.; van den Linden, J. G. M.; Roelofsen, A. M.; Jenneskens, L. W.; Drenth, W.; van Koten, G. *Organometallics* **1994**, *13*, 468.
[17] (a) Dahlhoff, W. V.; Nelson, S. M. *J. Chem. Soc. A* **1971**, 2184. (b) Hahn, C.; Spiegler, M.; Herdtweck, E.; Taube, R. *Eur. J. Inorg. Chem.* **1999**, 435. (c) Abbenhuis, R. A. T. M.; del Rio, I.; Bergshoef, M. M.; Boersma, J.; Veldman, M.; Spek, A. L.; van Koten, G. *Inorg. Chem.* **1998**, *37*, 1749. (d) Zhang, J.; Leitus, G.; Ben-David, Y.; Milstein, D. *J. Am. Chem. Soc.* **2005**, *127*, 10840.
[18] Heck, R. F. *J. Am. Chem. Soc.* **1968**, *90*, 5518.
[19] Takenaka, K.; Minakawa, M.; Uozumi, Y. *J. Am. Chem. Soc.* **2005**, *127*, 12273.
[20] Miyaura, M.; Suzuki, A. *Chem. Rev.* **1995**, *95*, 2457.
[21] Guillena, G.; Kruithof, C. A.; Casado, M. A.; Egmond, M. R.; van Koten, G. *J. Organomet. Chem.* **2003**, *668*, 3.
[22] Schrock, R. R. *Topics in Organometallic Chemistry* **1998**, *1*, 1.

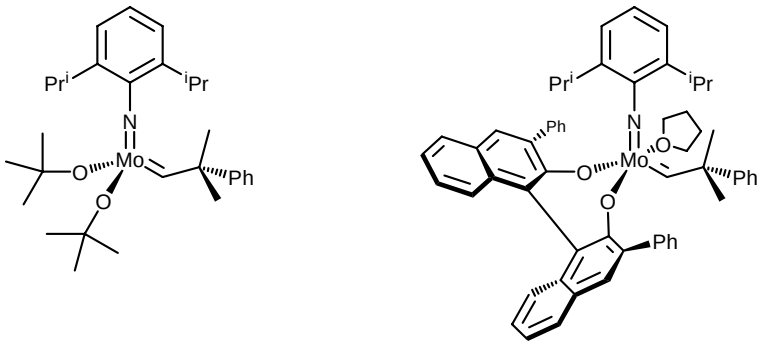

Figure 2.6 Examples for achiral (left) and chiral (right) Schrock catalysts

Molybdenum complexes are also known to catalyze olefin epoxidation, first reported in 1965[23]. In this early work MoO_2 was used to catalyze the epoxidation of an olefin with *tert*-butyl-peroxide. Later, readily prepared oxobisperoxo complexes were used which were first reported in 1969[24]. Thiel and coworkers for example developed oxobisperoxo molybdenum complexes (see Figure 2.7) with a high activity for the epoxidation in catalytic as well as in stoichiometric reactions[25]. Recently Hermann reported the first chiral epoxidation catalysts based on molybdenum[26]. All these compounds have in common that molybdenum is in high oxidation states.

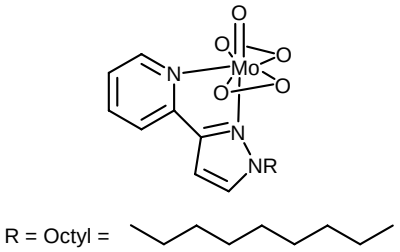

Figure 2.7 Example of an epoxidation catalyst

A recent application of organomolybdenum complexes is the fixation and activation of dinitrogen[27].

Another feature of molybdenum and tungsten complexes is their tendency to form stable seven-coordinated species, which is a quite rare geometry in transition-metal chemistry. There are four main types of structures exhibited for seven-coordinated complexes[28,29]: (i) capped octahedral,

---

[23] Indictor, N.; Brill, W. F. *J. Org. Chem.* **1965**, *30*, 2074.
[24] Mimoun, H.; Serée de Roch, I.; Sajus, L. *Bull. Soc. Chim.* **1969**, 1481.
[25] Thiel, W. R. *J. Mol. Cat. A* **1997**, *117*, 449.
[26] Kuehn, F. E.; Zhao, J.; Herrmann, W. A. *Tetrahedron: Asymmetry* **2005**, *16*, 3469.
[27] Schrock, R. R. *Acc. Chem. Res.* **2005**, *38*, 955.
[28] Melník, M.; Sharrock, P. *Coord. Chem. Rev.* **1985**, *65*, 49.
[29] Drew, M. G. B. *Prog. Inorg. Chem.* **1977**, *23*, 67.

(ii) capped trigonal prismatic, (iii) 4:3 or piano-stool geometry, and (iv) pentagonal bipyramidal geometry. Examples for tungsten complexes in all these geometries are given in Figure 2.8.

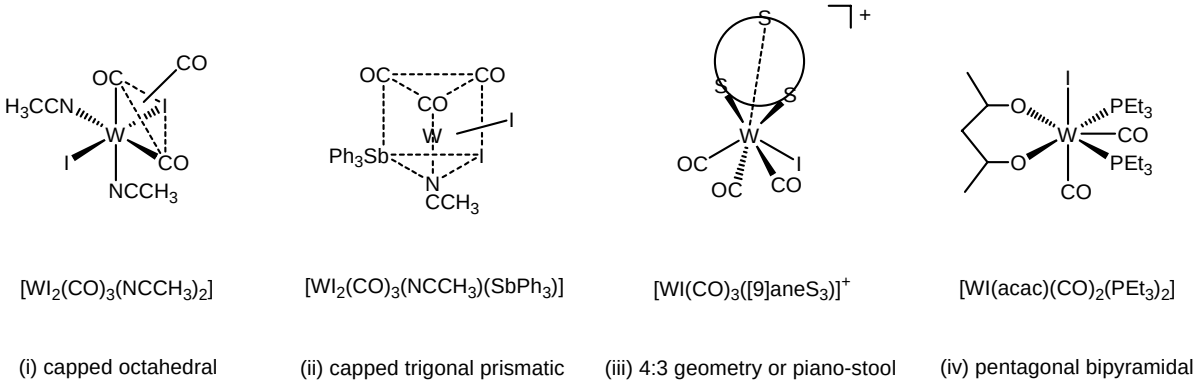

Figure 2.8 The four main geometries of seven-coordinated complexes

None of these geometries is energetically significantly favored and therefore the seven-coordinated complexes show fluxional behavior in solution.

Especially seven-coordinated halocarbonyl complexes of molybdenum and tungsten are versatile starting materials in synthetic chemistry[30]. Starting from complexes of the type $MXY(CO)_3(NCCH_3)$ (M = Mo, W; X, Y = Cl, Br, I) an immense variety of molybdenum and tungsten complexes can be prepared.

[30] Baker, P. K. *Chem. Soc. Rev.* **1998**, *27*, 125.

3 Results and Discussion

3.1 Preparation of the Ligand Building Blocks

The two chlorophosphites 2-chlorodibenzo[*d*,*f*]-1,3,2-dioxaphosphepine (BIPOL-PCl, **1a**) and 2-chloro-((4*R*,5*R*)-dicarbomethoxy-1,3,2-dioxaphospholane (TAR^{Me}-PCl, **1b**) were prepared as starting materials for the preparation of the phosphite based PNP ligands. Both chlorophosphites were prepared via a simple condensation reaction of PCl_3 and the corresponding diol using *N*-methylpyrrolidone (NMP) as catalyst (see Figure 3.1)[31,32].

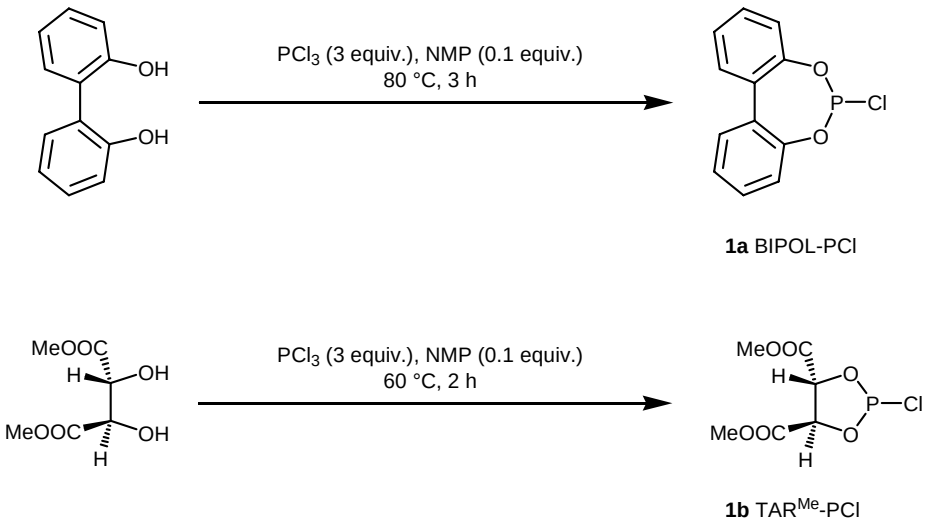

Figure 3.1 Preparation of the Chlorophosphites (**1a** and **1b**)

For the preparation of **1a**, 2,2'-biphenol, PCl_3, and NMP were added and the reaction mixture was stirred at 80 °C for 3 h (see Figure 3.1). **1b** was prepared analogously starting from PCl_3 and L-(+)-methyl tartrate.

While the formation of BIPOL-PCl (**4a**) needed elevated temperatures (80 °C), the formation of TAR^{Me}-PCl (**1b**) already started immediately after the addition of the tartrate to PCl_3 and NMP at 0 °C. The beginning of the reaction was indicated by the evolution of HCl. The elevated temperature (60 °C) was applied to guarantee complete conversion.

---

[31] (a) Tsarev, V. N.; Kabro, A. A.; Moieseev, S. K.; Kalinin, V. N.; Bondarev, O. G.; Davankov, V. A.; Gavrilov, K. N. *Russ. Chem. Bull., Int. Ed.* **2004**, *53*, 814. (b) van Rooy, A.; Kamer, P. C. J.; van Leeuwen, P. W. N. M.; Goubitz, K.; Fraanje, J.; Veldman, N.; Spek, A. *Organometallics* **1996**, *15*, 835.
[32] Kadyrov, R.; Heller, D.; Selke, R. *Tetrahedron: Asymmetry* **1998**, *9*, 329.

After the reactions were completed the excess of PCl_3 was removed under vacuum. The crude products were purified via bulb-to-bulb ("Kugelrohr") distillation that gave BIPOL-PCl (**1a**) and TARMe-PCl (**1b**) as colorless oils in 87 % and 80 % yield, respectively. **1a** crystallized during storage at reduced temperature (refrigerator, approx. 4 °C). The chlorophosphites are air and moisture sensitive and therefore had to be stored under argon.

Both products were characterized via ^{1}H and $^{31}P\{^{1}H\}$ NMR spectroscopy. The $^{31}P\{^{1}H\}$ NMR spectra exhibit single resonances at 180 (**1a**) and 175 (**1b**) ppm, respectively. This corresponds to a strong deshielding of the phosphorus atoms due to the electron withdrawing effect of the oxygen atoms. The ^{1}H NMR spectrum of BIPOL-PCl (**1a**) shows no characteristic signals. The aromatic protons give rise to a multiplet in the range from 7.58 – 7.22 ppm. The ^{1}H NMR spectrum of TAR^{Me}-PCl (**1b**) shows a doublet at 5.57 ppm (J = 6.2 Hz) and a doublet of doublet at 4.79 ppm (J = 6.2 Hz, J_{PH} = 9.8 Hz) of the 1,3,2-dioxaphospholane protons and two single resonances at 3.33 and 3.24 ppm for the methyl groups due to the chirality of the compound.

3.2 Preparation of the Ligands

PNP ligands known to literature are mostly alkyl bridged ligands. One method for the synthesis of those pincer ligands developed by Shaw requires 1,3-dimethylbenzene as starting material, which is radically halogenated with N-bromosuccinimide first. The 2,6-bis(bromomethyl)-benzene is nucleophilically attacked by 2 equiv. of $LiPR_2$ to give the desired methyl-bridged PCP pincer-ligand. This synthetic strategy also works with 2,6-dimethylpyridine as starting material to gain PNP pincer ligands. The general reaction scheme is shown in Figure 3.2.

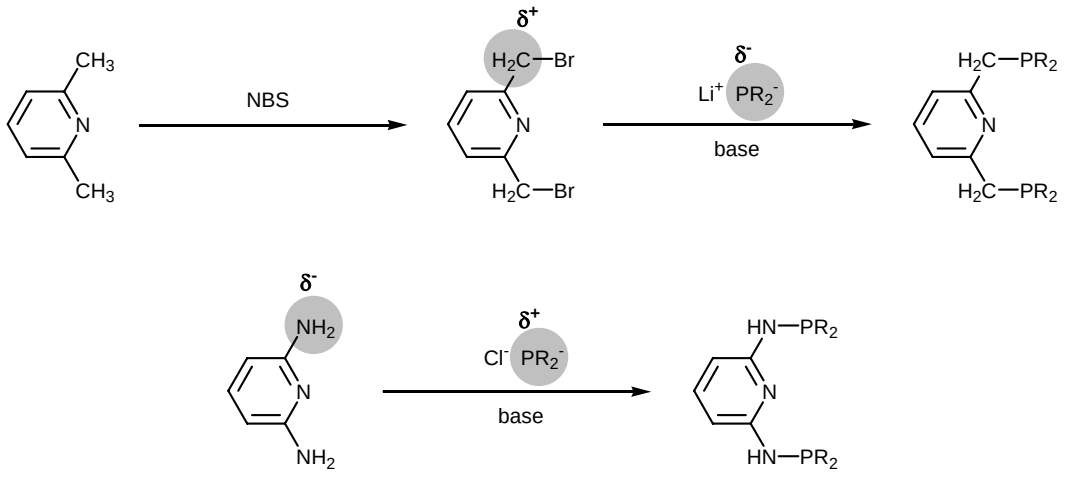

Figure 3.2 Comparison of the synthetic routes to alkyl- and amino-bridged PNP ligands

In this work, amino-bridged PNP pincer ligands were used. In contrast to the alkyl carbon the amino group has a negative partial charge. Due to the inverted polarity phosphine- and phosphite-

donors can be introduced as electrophiles using the corresponding chlorophosphines and -phosphites, respectively. Besides the fact that 2,6-diaminopyridine and chlorophosphines are commercially available and cheap, this methodology requires only one step to gain pincer ligands. This makes the synthesis much easier and faster and with the cheaper starting materials overall more economic.

This in turn results in a system of modularly designed pincer ligands with various substituents at the phosphorus atom. Electronic and steric properties can be modified easily. Switching from phosphines to phosphites widens the field of electronic properties and also opens another interesting option: an easy way to introduce chirality via the use of phosphite donors based on chiral diols. These chiral ligands and complexes thereof are of great interest in the field of asymmetric catalysis.

It has to be noted that the principle of the reverse of polarity also is applicable for oxygen bridged PCP pincer ligands[33,34]. In the case of PNP pincer ligands based on 2,6-dihydroxypyridine this method does not result in the desired products, because the deprotonation of the second oxygen fails due to the tautomeric stabilization of a hydroxypyridinone species (see Figure 3.3).

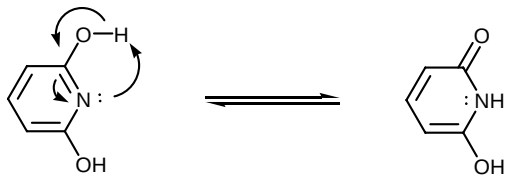

Figure 3.3 Tautomerism between 1,3-dihydroxypyridine and 6-hydroxypyridin-2-one

Substitution of the aromatic backbone of the pincer ligand is an efficient way to increase the solubility and therefore is a useful tool for catalytic applications. The substituent on the aromatic moiety does not change the electronic behavior of the ligand very much and thus does not influence the binding to the metal center[35].

In this research group also 2,6-diamino-4-phenyl-1,3,5-triazine has been used as an alternative aromatic backbone to synthesize PNP ligands analogously to the pyridine-based PNP ligands (see Figure 3.4). In addition PNP ligands with alkylated amino-bridges have been synthesized (see Figure 3.4)[5,36].

[33] Morales-Morales, D.; Redón, R.; Yung, C.; Jensen, C. M. *Inorg. Chim. Acta* **2004**, *357*, 2953.
[34] Goettker-Schnetmann, I.; White, P.; Brookhart, M. *J. Am. Chem. Soc.* **2004**, *126*, 1804.
[35] Bocokić, V. *Diploma Thesis*, TU Wien **2006**.
[36] Pollak, M. *Diploma Thesis*, TU Wien **2006**.

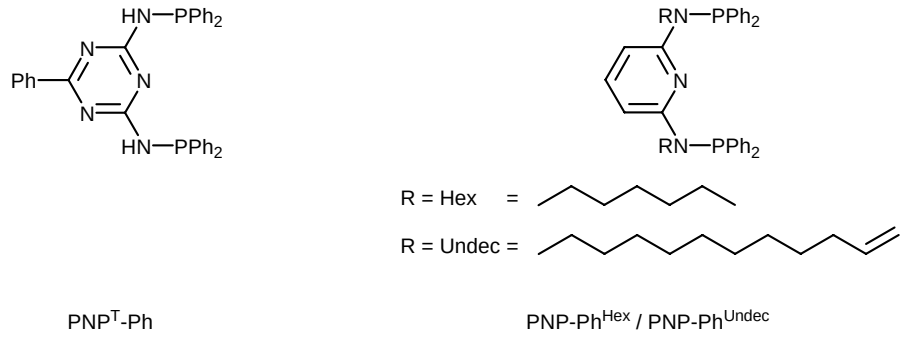

Figure 3.4 Triazine-based and N-alkylated amino-bridged PNP pincer ligands

In this work a special notation for the ligands is used, additionally indicating the substituents at the phosphorus atoms via a suffix, e.g. -TAR^{Me} for L-(+)-tartrate or -BIPOL for 2,2'-biphenol.

The PNP ligands were prepared in a simple one step synthesis. 2,6-diaminopyridine was used as starting material and reacted with the respective chlorophosphines or -phosphites. The chlorophosphines or -phosphites were added to a solution of 2,6-diaminopyridine and triethylamine in toluene at 0 °C, and the reaction mixture was stirred at 80 °C for 18 h (see Figure 3.5). During the reaction triethylammmonium chloride precipitated as a white solid.

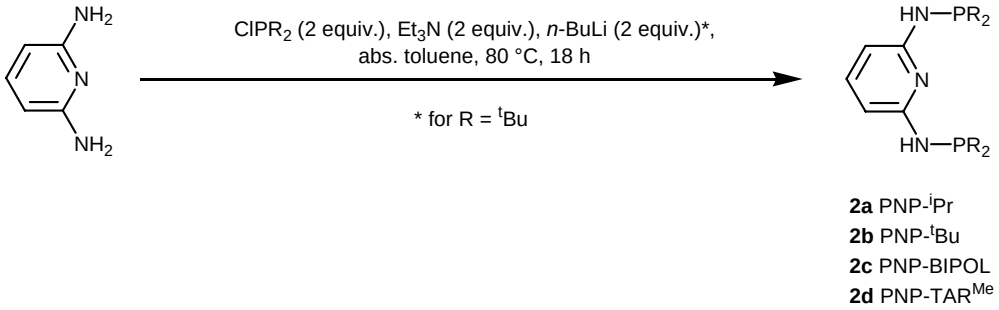

Figure 3.5 Preparation of the PNP ligands (**2a-d**)

The synthesis of PNP-^{t}Bu (**2b**) required a stronger base than triethylamine because the tertiary-butyl substituents are not only bulky but also have a stronger positive inductive effect and therefore make the phosphorus less electrophilic. Monitoring the reaction of 2,6-diaminopyridine in the presence of triethylamine and chlorodi-*tert*-butylphosphine in toluene via $^{31}P\{^1H\}$ NMR spectroscopy clearly showed that no reaction took place and only the resonance of the chlorodi-*tert*-butylphosphine at 149 ppm was observed. For this reason the reaction mixture was cooled to -80 °C and 2 equiv. of *n*-butyllithium were added. Then the reaction mixture was heated to 80 °C. Now the formation of the desired product could be observed by the appearance of a single resonance at 58 ppm and the disappearance of the educt signal, but also the formation of a byproduct, which was identified as

n-butyl-di-*tert*-butylphosphine was observed[37]. The formation of this byproduct can be prevented by adding *n*-butyl lithium to the reaction mixture and allow a complete deprotonation of the amino functionalities before the addition of the chlorophosphine.

Based on these results the procedure for the preparation of **2b** was modified. The mixture of 2,6-diaminopyridine and triethylamine was cooled to -80 °C and 2 equiv. of *n*-butyl lithium were added. The reaction mixture was warmed to room temperature and stirred for 2 h. Chlorodi-*tert*-butylphosphine was added and the reaction mixture stirred at 80 °C for 18 h.

All ligands were worked up by filtration to remove the formed ammonium salt and evaporation of the solvent. PNP-^{i}Pr (**2a**) was not further purified and obtained in 97 % yield. PNP-^{t}Bu (**2b**), PNP-BIPOL (**2c**), and PNP-TAR^{Me} (**2d**) were purified by recrystallization from toluene/*n*-hexane (1:1) and obtained in 54, 84 and 74 % yield, respectively.

The ligands were characterized via ^{1}H, ^{31}P{^{1}H}, and ^{13}C{^{1}H} NMR spectroscopy. Some characteristic ^{1}H and ^{31}P NMR resonances are given in Table 3.1.

Table 3.1 Selected ^{1}H and ^{31}P{^{1}H} NMR resonances of the PNP ligands

		^{31}P{^{1}H} (δ [ppm], $CDCl_3$, 20 °C)	**^{1}H (δ [ppm], $CDCl_3$, 20 °C)**		
			py^{4} (1H)	py^{3,5} (2H)	N*H* (2H)
2a	PNP-^{i}Pr	49.0	7.23 (t)	6.42 (dd)	4.29 (d)
2b	PNP-^{t}Bu	60.2	7.25 (t)	6.48 (dd)	4.64 (d)
2c	PNP-BIPOL	147.2	*	5.89 (d)	4.32 (bs)
2d	PNP-TAR^{Me}	142.9	7.30 (t)	6.28 (d)	6.45 (s)

* resonance overlaps with signals of biphenyl-rings

The ^{31}P{^{1}H} NMR spectra show resonances for the phosphines (**2a** and **2b**) at 49.0 and 60.2 ppm, respectively. The spectra of the phosphites (**2c** and **2d**) clearly show the deshielding effect of the oxygen atoms, exhibiting resonances at 147.2 and 142.9 ppm respectively.

The ^{1}H NMR spectra of all ligands show characteristic resonances of the pyridine protons in the range of 7.30 – 7.23 ppm (py^{4}) and 6.48 – 5.89 ppm (py^{3,5}). The resonances of the amino protons appear in the range of 4.64 – 4.29 ppm for **2a-c**. The resonance of the amino protons of **2d** is shifted to the low field as a result of hydrogen bridges between the amino hydrogen atoms and the carboxylic groups. The ^{1}H NMR spectrum of PNP-^{i}Pr (**2a**) shows in addition to the resonances given in Table 3.1 two resonances for the CH and CH_3 groups of the isopropyl substituents at 1.08 – 0.99 and 1.78 – 1.67 ppm, respectively. PNP-^{t}Bu (**2b**) exhibits a multiplet resonance at 1.22 – 1.15 ppm corresponding to the CH_3 groups of the *tert*-butyl substituents.

[37] Samuel, G. O.; Yankowsky, A. W.; Salvatore, B. A.; Bailey, W. J.; Davidoff, E. F.; Marks, T. J. *Journal of Chemical and Engineering Data* **1970**, *15*, 497.

In the ^{1}H NMR spectrum of PNP-BIPOL (**2c**) a shift of some of the biphenyl hydrogen atoms to the high field in comparison to the chlorophosphite can be observed. The spectrum exhibits resonances at 6.40 (d, J = 7.8 Hz, 4H, Ph^{4}) and 6.11 (dd, J = 31.6 Hz, J = 7.8 Hz, 4H, Ph^{6}) compared to 7.58 and 7.22 ppm in the ^{1}H NMR spectrum of **1a**. Interestingly, the resonances of the py^{3,5} hydrogen atoms are shifted to the high field compared to those of the other three ligands (compare Table 3.1). The ^{1}H NMR spectrum of PNP-TAR^{Me} (**2d**) exhibits resonances of the dioxaphospholane protons at 5.06 – 5.03 and 4.81 – 4.75 ppm, respectively. The CH_3 groups exhibit one resonance at 3.83 ppm and are not distinguishable like in the chlorophosphite **1b**.

The ^{13}C{^{1}H} NMR spectra of the ligands **2a –d** show resonances for the pyridine carbon atoms in the range of 159.5 – 153.8 (py^{2,6}), 140.0 – 138.7 (py^{4}), and 101.9 – 98.1 ppm (py^{3,5}), respectively. The py^{2,6} and py^{3,5} atoms show doublet resonances as a result of C-P coupling with coupling constants J_{PC} between 10.3 and 20.3 Hz. The ^{13}C{^{1}H} NMR spectra of **2a** and **2b** show resonances of the substituents at the phosphorus in the range between 29.4 and 17.3 ppm with J_{PC} between 7.7 and 19.6 Hz. The ^{13}C{^{1}H} NMR spectrum of **2c** exhibits resonances for the aromatic carbon atoms in the range of from 149.5 to 122.3 ppm. In the ^{13}C{^{1}H} NMR spectrum of **2d** two characteristic resonances for the carbonyl groups can be observed at 171.3 and 169.0 ppm.

3.3 Preparation of the Molybdenum and Tungsten Precursors

3.3.1 Preparation of the Tricarbonyltris(acetonitrile) and Tetracarbonylbis(acetonitrile) Precursors

The tricarbonyltris(acetonitrile) complexes $Mo(CO)_3(NCCH_3)_3$ (**3a**) and $W(CO)_3(NCCH_3)_3$ (**3a'**) were used as starting materials for the syntheses of the molybdenum and tungsten pincer complexes. These precursors were prepared according to a method published by Augl and coworkers[38].

The three carbonyl and three acetonitrile ligands of **3a** and **3a'**, respectively, are coordinated in a facial arrangement. This is a result of the fact that CO ligands situated trans to acetonitrile ligands are bound stronger to the metal center, because acetonitrile is a stronger σ-donor and weaker π-acceptor and therefore strengthens especially the π-backdonation between the metal center and the CO ligand situated trans[39]. Thus, CO ligands trans to other CO ligands can be replaced easier. The trans effect is also the reason why the substitution of the CO ligands does not prolong after the exchange of the first three ligands, because the remaining CO ligands are bound too strongly to be replaced by acetonitrile.

[38] Tate, D. P.; Knipple, W. R.; Augl, J. M. *Inorg. Chem.* **1962**, *1*, 433.
[39] Stolz, I. W.; Dobson, G. R.; Sheline, R. K. *Inorg. Chem.* **1963**, *2*, 323.

The better σ-donor properties of the acetonitrile ligands also strengthen the binding of the CO ligands to the metal center coordinated cis because of the increase of the electron density of the metal center. Therefore also the π-backdonation from the metal center to these CO ligands is increased, but not to the degree as for the CO ligands coordinated trans to the acetonitrile ligands.

As a result of these electronic effects the formation of the molybdenum and tungsten tricarbonyltris(acetonitrile) complexes proceeds via subsequent release of three CO ligands. The separation of the third CO is much more difficult than that of the first two, and therefore the tetracarbonylbis(acetonitrile) complex can also be prepared cleanly via a adaptation of the reaction conditions.

For the preparation of **3a**, molybdenumhexacarbonyl was refluxed in acetonitrile under inert atmosphere (argon) for 4 h. Afterwards the yellow solution was cooled to room temperature (see Figure 3.6). $W(CO)_3(NCCH_3)_3$ (**3a'**) was prepared analogously, but tungstenhexacarbonyl was used as starting material and the reaction time had to be extended to 7 d because of the lower reactivity of $W(CO)_6$.

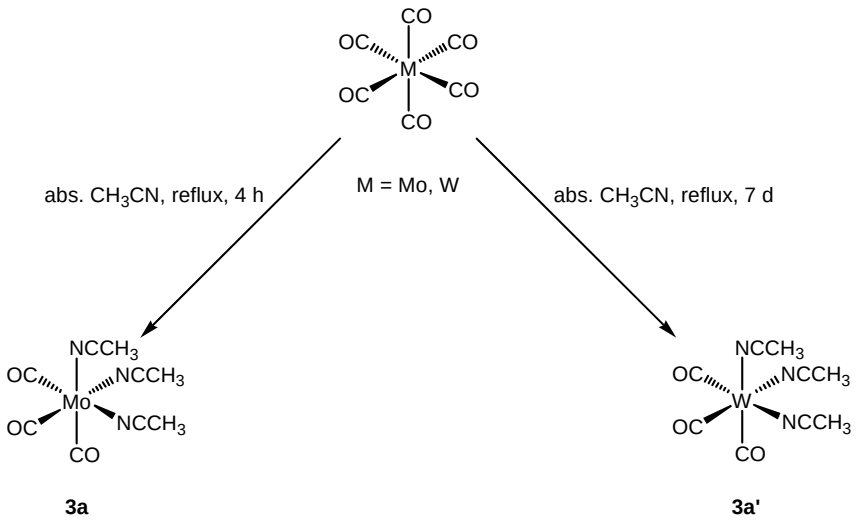

Figure 3.6 Preparation of $M(CO)_3(NCCH_3)_3$ (M = Mo, W) (**3a** and **3a'**)

As a result of the highly air and moisture sensitivity of **3a',** undesired byproducts were formed during the long reaction time. With one exception (**6a'**) the subsequent syntheses of PNP Pincer complexes starting from **3a'** failed.

$Mo(CO)_4(NCCH_3)_2$ (**3b**) was prepared by shortening the reaction time from 4 to 3 h and lowering the reaction temperature from 85 to 70 °C (see Figure 3.7).

Compounds **3a**, **3a'**, and **3b** are highly air and moisture sensitive yellow solids and therefore were used without isolation and characterization.

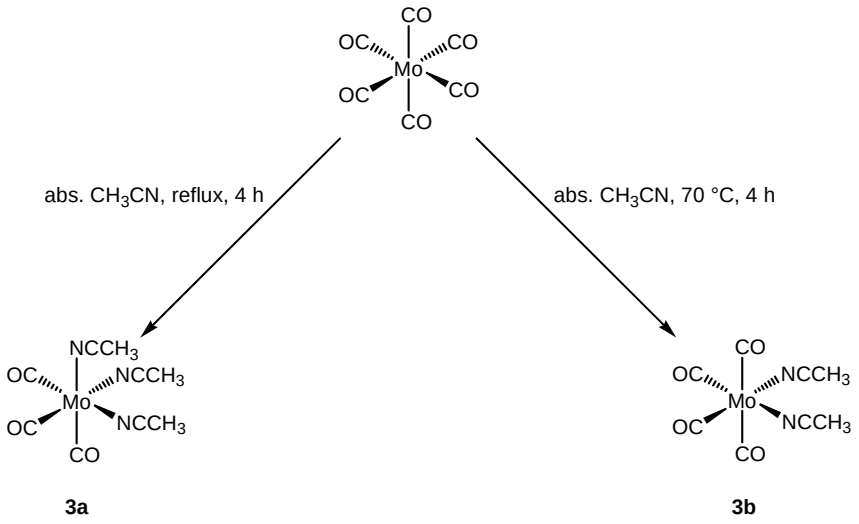

Figure 3.7 Preparation of *mer*-$Mo(CO)_3(NCCH_3)_3$ (**3a**) and *cis*-$Mo(CO)_4(NCCH_3)_2$ (**3b**)

3.3.2 $MoI_2(CO)_3(NCCH_3)_2$

$MoI_2(CO)_2(NCCH_3)_2$ (**4**) was prepared to provide an alternative molybdenum precursor to prepare halocarbonyl pincer complexes. **4** and analogous seven-coordinated halocarbonyl complexes of molybdenum and tungsten are well known and used as versatile starting materials in a lot of different syntheses[40,41]. The geometry of the complex $MoI_2(CO)_2(NCCH_3)_2$ (**4**) could be described as a capped octahedron (see Chapter 2.3 and Figure 2.8).

For the preparation of **4**, 1 equiv. of iodine was added to *in situ* prepared $Mo(CO)_3(NCCH_3)_3$ (**3a**) (see Chapter 3.3.1) at 0 °C whereas the color of the reaction mixture immediately changed to dark red (see Figure 3.8). The reaction mixture was stirred for 1 h at room temperature, the solvent was evaporated and the a red brown solid obtained in 90 % yield. The complex was stored under argon because of its limited air stability[42].

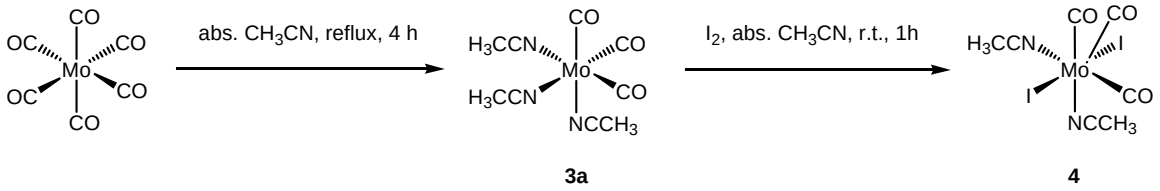

Figure 3.8 Preparation of $MoI_2(CO)_2(NCCH_3)_2$ (**4**)

[40] Balakrishna, M. S.; Krishnamurthy, S. S.; Manohar, H. *Organometallics* **1991**, *10*, 2522.
[41] Cano, M.; Campo, J. A.; Heras, J. V.; Pinilla, E.; Monge, A. *Polyhedron* **1996**, *15*, 1705.
[42] Baker, P. K.; Meehan, M. M.; Kwen, H.; Abbott, A. *Inorg. Synth.* **2002**, *33*, 239.

The product was characterized via ATR-IR-spectroscopy. The IR spectrum exhibited two nitrile resonances at 2304 (m) and 2277 (m) cm^{-1} and two carbonyl resonances at 2015 (s) and 1918 (s) cm^{-1}. The third predicted CO resonance is only observable as a shoulder of the signal at 2015 cm^{-1}.

3.3.3 $Mo(\eta^3\text{-allyl})(CO)_2(NCCH_3)_2Br$

$Mo(\eta^3\text{-allyl})(CO)_2(NCCH_3)_2Br$ (**5**) is a well known compound first synthesized by Friedel and coworkers in 1968[43]. In this work it was prepared as alternative precursor for complexation reactions with the PNP ligands.

1 equiv. of allyl bromide was added to *in situ* prepared $Mo(CO)_3(NCCH)_3$ (**3a**) (see Chapter 3.3.1) whereas effervescence could be observed and an orange precipitate was formed (see Figure 3.9). The solution was warmed to room temperature and the reaction mixture was stirred until no more effervescence could be observed when the flask was purged with argon (6 d). The solvent was evaporated and the obtained orange solid used without further purification and characterization.

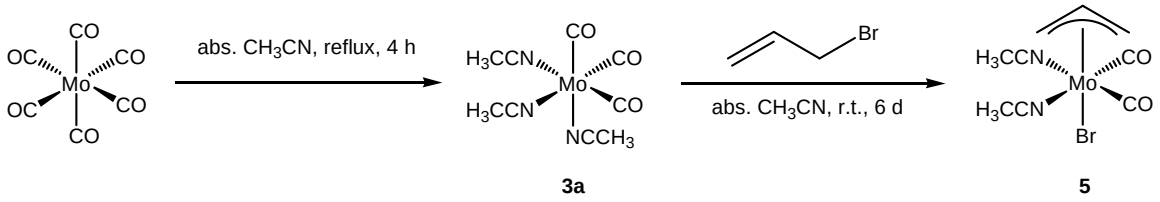

Figure 3.9 Preparation of $Mo(\eta^3\text{-allyl})(CO)_2(NCCH_3)_2Br$ (**3**)

3.4 Preparation of the Pincer Complexes

3.4.1 Tricarbonyl Complexes

Molybdenum and tungsten tricarbonyl PNP pincer complexes are easily accessible by a ligand exchange reaction between **3a** or **3a'** and a corresponding PNP ligand. For the formation of the pincer complexes the coordination geometry of the three carbonyl ligands at the metal center has to change from a facial to a meridional arrangement.

For the preparation of molybdenum tricarbonyl PNP pincer complexes, *in situ* prepared $Mo(CO)_3(NCCH_3)_3$ (**3a**) (see Chapter 3.3.1) was reacted at room temperature with 1 equiv. of a PNP ligand at room temperature (see Figure 3.10). Acetonitrile was used as solvent, which did not cause problems since the coordination of the PNP ligand is much stronger than that of acetonitrile. After a

[43] Tom Dieck, H.; Friedel, H.; *J. Organomet. Chem.* **1968**, *14*, 375.

reaction time of 18 h the solvent was evaporated and the complexes were purified via column chromatography over neutral Al_2O_3. Mo(PNP-^{i}Pr)(CO)$_3$ (**6a**) and Mo(PNP-^{t}Bu)(CO)$_3$ (**6b**) were isolated as yellow and brown solids in 62 % and 15 % yield, respectively.

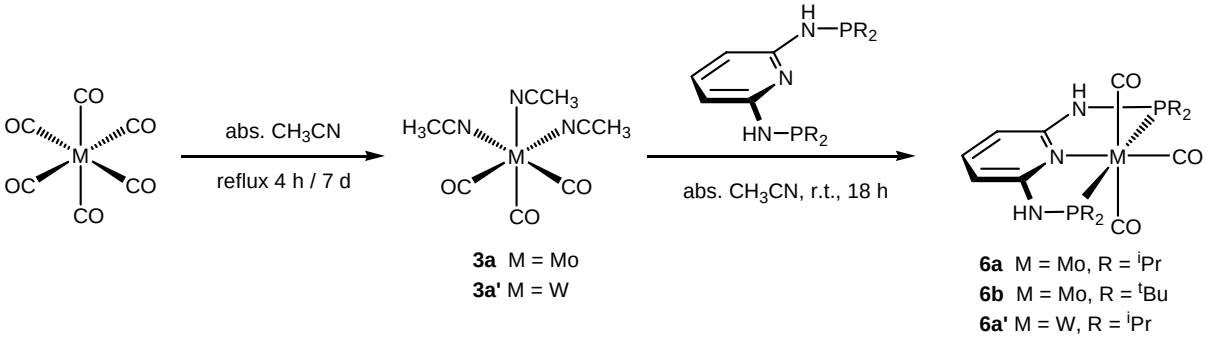

Figure 3.10 Preparation of the tricarbonyl pincer complexes (**6a**, **6a'**, and **6b**)

The preparation of the analogous complexes starting from PNP-BIPOL (**2c**) and PNP-TAR^{Me} (**2d**) failed, resulting in product mixtures which could not be separated.

W(PNP-^{i}Pr)(CO)$_3$ (**6a'**) was prepared analogously starting from W(CO)$_3$(NCCH$_3$)$_3$ (**3a'**) as precursor, but a longer reaction time was necessary. Due to the long reaction time byproducts were formed which were separated via column chromatography. **6a'** was obtained as yellow solid in 6 % yield.

The complexes showed limited air stability in solution. In the solid state the stability was better, but longer exposure to air also caused degradation. Therefore the products had to be stored under argon.

All products were characterized via ^{1}H, ^{31}P{^{1}H} and ^{13}C{^{1}H} NMR spectroscopy. Some characteristic ^{1}H and ^{31}P{^{1}H} NMR resonances are given in Table 3.1.

Table 3.2 Selected ^{1}H and ^{31}P{^{1}H} NMR resonances of the tricarbonyl PNP pincer complexes

		solvent	^{31}P{^{1}H} (δ [ppm], 20 °C)	^{1}H (δ [ppm], 20 °C)		
				py^4 (1H)	py^{3,5} (2H)	N*H* (2H)
6a	Mo(PNP-^{i}Pr)(CO)$_3$	CD_3CN	131.9	7.16 (t)	6.13 (d)	6.37 (bs)
6b	Mo(PNP-^{t}Bu)(CO)$_3$	CD_2Cl_2	148.8	7.18 (t)	6.13 (d)	5.25 (bs)
6a'	W(PNP-^{i}Pr)(CO)$_3$	$CDCl_3$	117.8	7.10 (t)	6.09 (d)	5.39 (bs)

The comparison of the ^{31}P{^{1}H} NMR resonances of **6a** and **6a'** shows that tungsten has a less electron withdrawing effect and therefore the phosphorus atoms are less deshielded, resulting in a resonance at 117.8 ppm for the tungsten complex **6a'** compared to 131.9 ppm for the molybdenum

complex **6a**. Analogously to the ligands, the resonance of **6b** is shifted to the low field compared to **6a** (148.8 compared to 131.9 ppm).

The ^{1}H NMR spectra exhibit characteristic signals analogous to the spectra of the ligands and with comparable shifts (compare Table 3.3). The resonances of the amino hydrogen atoms show a dependence on the solvent. This is a result of the acidity of the amino hydrogen atoms, which form hydrogen bridges to polar solvent molecules and are thus deshielded. Therefore more polar solvents cause resonances shifted to the low field (6.37 ppm for **6a** in CD_3CN compared to 5.25.ppm for **6b** in CD_2Cl_2).

In the $^{13}C\{^{1}H\}$ NMR spectra two additional resonances for the three carbonyl ligands can be observed in the range between 235 and 205 ppm. The two carbonyls perpendicular to the PNP ligand are equivalent and show only one resonance in the $^{13}C\{^{1}H\}$ NMR spectra. Both carbonyl resonances are triplets due to their coupling with the two equivalent phosphorus atoms. **6a** shows resonances in the $^{13}C\{^{1}H\}$ NMR spectrum at 231.4 (t, J_{PC} = 5.8 Hz) and 216.9 ppm (t, J_{PC} = 10.4 Hz) for the CO ligands. The pyridine carbons show resonances at 161.0 (t, J_{PC} = 10.4 Hz, $py^{2,6}$), 137.7 (py^{4}), and 97.1 ppm (t, J_{PC} = 3.1 Hz, $py^{3,5}$), respectively. The $^{13}C\{^{1}H\}$ NMR spectra of **6b** and **6a'** show analogous patterns with only minor shifts of the resonances to the high or low field. All complexes exhibit resonances for the substituents at the phosphorus in the range from 39.9 to 17.8 ppm, showing C-P coupling (J_{PC} = 3.0 -10.4 Hz).

Table 3.3 Comparison of selected ^{1}H and $^{31}P\{^{1}H\}$ NMR resonances of the PNP ligands and their molybdenum tricarbonyl complexes

		solvent	$^{31}P\{^{1}H\}$ (δ [ppm], 20 °C)	^{1}H (δ [ppm], 20 °C)		
				py^{4} (1H)	$py^{3,5}$ (2H)	N*H* (2H)
2a	PNP-^{i}Pr	$CDCl_3$	49.0	7.23 (t)	6.42 (dd)	4.29 (d)
6a	Mo(PNP-^{i}Pr)$(CO)_3$	CD_3CN	131.9	7.16 (t)	6.13 (d)	6.37 (bs)
2b	PNP-^{t}Bu	$CDCl_3$	60.2	7.25 (t)	6.48 (dd)	4.64 (d)
6b	Mo(PNP-^{t}Bu)$(CO)_3$	CD_2Cl_2	148.8	7.18 (t)	6.13 (d)	5.25 (bs)

Table 3.3 compares the ^{1}H and $^{31}P\{^{1}H\}$ NMR resonances of the complexes **6a** and **6b** to their corresponding free ligands **2a** and **2b**. The resonances of the $^{31}P\{^{1}H\}$ NMR spectra show a shift of about 80 – 90 ppm from 49.0 to 131.9 ppm (**6a**) and 60.2 to 148.8 (**6b**) ppm for the resonances of the complexes, corresponding to a strong deshielding of the phosphorus atoms caused by the coordination to the metal center.

The resonances for the pyridine protons in the ^{1}H NMR spectra are slightly shifted to the high field. In contrast, the signal of the CH groups of the isopropyl substituents of **6a** shifts from 1.78 – 1.67 to

2.45 – 2.18 ppm to the low field. The resonances of the CH_3 groups of the isopropyl and *tert*-butyl substituents of **6a** and **6b** do not show a significant shift compared to the signals of the ligands.

3.4.2 Tetracarbonyl Complexes

An interesting result of this work was the development of a synthetic route to molybdenum tetracarbonyl PNP pincer complexes. These complexes are not pincer complexes strictly speaking, because the ligands are only binding in a bidentate mode.

$Mo(CO)_4(NCCH_3)_2$ (**3b**) was prepared (see Chapter 3.3.1) and reacted *in situ* with a corresponding PNP ligand (**2a** or **2b**) at room temperature in acetonitrile (see Figure 3.11). After 18 h the solvent was evaporated and the complexes were purified via column chromatography over neutral Al_2O_3. The complexes $Mo(PN(P)\text{-}^{i}Pr)(CO)_4$ (**7a**) and $Mo(PN(P)\text{-}^{t}Bu)(CO)_4$ (**7b**) were obtained as bright yellow solids in 58 % and 27 % yield, respectively (in this notation the brackets around the second P indicate that only one of the phosphorus atoms is coordinated to the metal center).

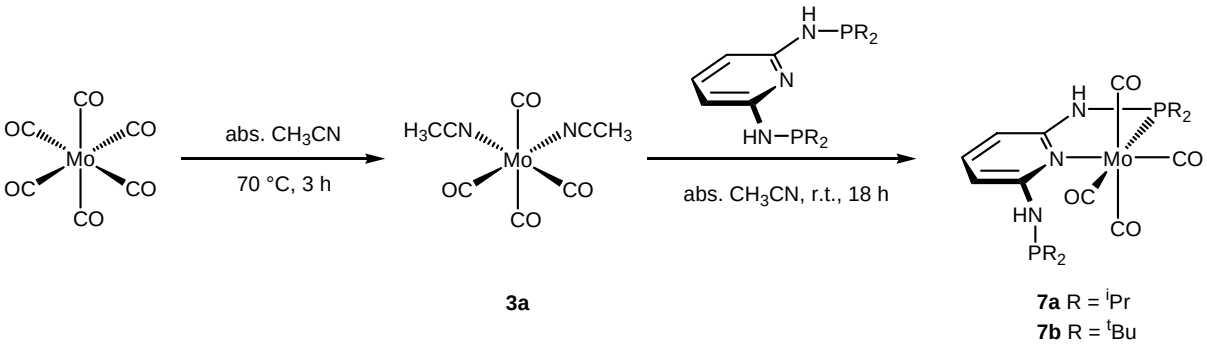

Figure 3.11 Preparation of the tetracarbonyl pincer complexes (**7a** and **7b**)

The products were characterized via ^{1}H, $^{31}P\{^{1}H\}$ and $^{13}C\{^{1}H\}$ NMR spectroscopy. In the $^{31}P\{^{1}H\}$ NMR spectra the non-equivalence of the two phosphorus atom can be observed easily (compare Table 3.4), exhibiting resonances at 110.7 and 56.7 ppm (**7a**) and 126.2 and 71.5 ppm (**7b**), respectively. As expected, the resonance of the non-coordinated phosphorus atom is located in the range of the free ligand (**2a**, 49.0 ppm and **2b**, 60.2 ppm) and the resonance of the coordinated phosphorus atom in the range of the tricarbonyl complex (**6a**, 131.9 ppm and **6b**, 148.8 ppm). Both resonances are located between the signals of the free ligand and the tricarbonyl complex, respectively.

Table 3.4 Comparison between the $^{31}P\{^{1}H\}$ NMR resonances of the tricarbonyl complexes, tetracarbonyl complexes, and free ligands

	$^{31}P\{^{1}H\}$ (δ [ppm], 20 °C)						
	Tricarbonyl complexes		**Tetracarbonyl complexes**			**Free ligand**	
				Coordinating	Non-coordinating		
^{i}Pr	**6a**	131.9[1)]	**7a**	110.7[1)]	56.7[1)]	**2a**	49.0[2)]
^{t}Bu	**6b**	148.8[3)]	**7b**	126.2[4)]	71.5[4)]	**2b**	60.2[2)]

solvents: [1)] CD_3CN, [2)] $CDCl_3$, [3)] CD_2Cl_2, [4)] d_6-acetone

The ^{1}H NMR spectrum of **7b** also shows a splitting of some signals into signals of the coordinating and non-coordinating "arm" of the ligand. The amino hydrogen atoms exhibit separate resonances at 7.01-6.86 (overlap with $py^{3,5}$) and 6.18 ppm and the $py^{3,5}$ protons (7.01-6.86 and 6.18 ppm) and the *tert*-butyl groups (1.41 and 1.26 ppm) also exhibit two resonances. In the ^{1}H NMR spectrum of **7a** all resonances – except the resonances of the py^{4} atoms and the CH_3 groups of the isopropyl substituents – analogously split into two resonances.

The $^{13}C\{^{1}H\}$ NMR spectrum of **7a** shows three CO resonances at 219.0, 213.2, and 206.2 ppm respectively, all triplets with coupling constants J_{PC} of about 10 Hz. The resonances for the pyridine carbon atoms can be found at 158.4 – 157.7 ($py^{2,6}$), 135.0 (py^{4}), 97.0 ($py^{3,5}$), and 95.8 ($py^{3,5}$). The isopropyl groups exhibit resonances at 29.7 and 28.1 ppm for the CH group and between 28.3 and 15.4 ppm for the CH_3 groups. **7b** shows an analogous pattern for the aromatic carbons and two resonances of the $C(CH_3)_3$ at 38.2 and 34.1 ppm, respectively and for the $C(CH_3)$ atoms four resonances between 28.4 and 27.9 ppm.

Additional experiments showed that it is possible to convert the tetracarbonyl complex $Mo(PN(P))(CO)_4$ (**7**) into the corresponding tricarbonyl complexes $Mo(PNP)(CO)_3$ (**6**) by heating the tetracarbonyl complex in acetonitrile to 60 °C for 5 h.

The synthesis of the tricarbonyl pincer complexes **6a** and **6b** was also carried out via a different route. $Mo(CO)_6$ was not converted to $Mo(CO)_3(NCCH_3)_3$ (**3a**) first but reacted directly with the corresponding PNP ligand in acetonitrile. If the preparation is done this way, the formation of $Mo(PN(P))(CO)_4$ as an intermediate could be observed by monitoring the reaction via $^{31}P\{^{1}H\}$ NMR spectroscopy.

3.5 Reactions of the Pincer Complexes

Mo(PNP-^{i}Pr)(CO)$_3$ (**6a**) was reacted with different substrates to study its reactivity in key reactions like oxidative addition or ligand exchange.

3.5.1 Reactions with Halogens

[Mo(PNP-^{i}Pr)(CO)$_3$I]I (**8a**) was prepared by reacting Mo(PNP-^{i}Pr)(CO)$_3$ (**6a**) with iodine in methylene chloride (see Figure 3.12). **6a** was dissolved in methylene chloride and iodine was added, whereupon the color of the reaction mixture changed from yellow to dark red. After 1 h of reaction time at room temperature the solvent was evaporated and the product was isolated as a dark red solid in 97 % yield.

For the preparation of [Mo(PNP-^{i}Pr)(CO)$_2$(NCCH$_3$)I]I (**8b**) the same starting materials were used, but acetonitrile was used as the solvent instead of methylene chloride (see Figure 3.12). After the addition of iodine, the mixture changed its color to dark red and a yellow solid precipitated. The reaction mixture was stirred at room temperature for 18 h. The precipitate changed its color from yellow to dark red during the reaction. The solvent was evaporated and the product isolated without further purification. The product was obtained as a dark red solid in 98 % yield.

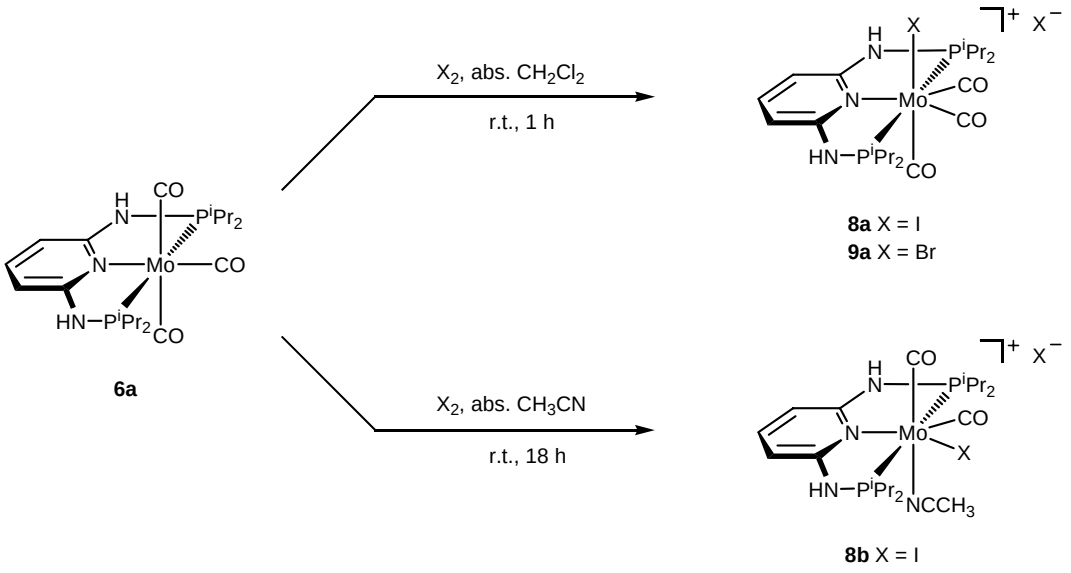

Figure 3.12 Reaction of Mo(PNP-^{i}Pr)(CO)$_3$ (**6a**) with halogens

[Mo(PNP-^{i}Pr)(CO)$_3$Br]Br (**9a**) was prepared analogously to **8a** using bromine instead of iodine. The product was not further purified and obtained as an orange solid in 94 % yield.

[Mo(PNP-^{i}Pr)(CO)$_3$I]I (**8a**) was also reacted with $AgSbF_6$ to exchange the counterion. **8a** was prepared and reacted *in situ* in methylene chloride with $AgSbF_6$ to give [Mo(PNP-^{i}Pr)(CO)$_3$I](SbF$_6$)

(**8a'**). After 3 h of reaction time at room temperature the formed AgI was filtered off and the solvent was evaporated. The product was isolated without further purification in 97 % yield.

8a was also prepared via an alternative synthetic route starting from $MoI_2(CO)_3(NCCH_3)_2$ (**4**) and PNP-^{i}Pr (**2a**) (see Figure 3.13). The ligand **2a** was added to the dark red solution of **4** in d_2-methylene chloride at room temperature. After 1 h the formation of **8a** was confirmed via ^{1}H and ^{31}P{^{1}H} NMR spectroscopy. The product was not isolated.

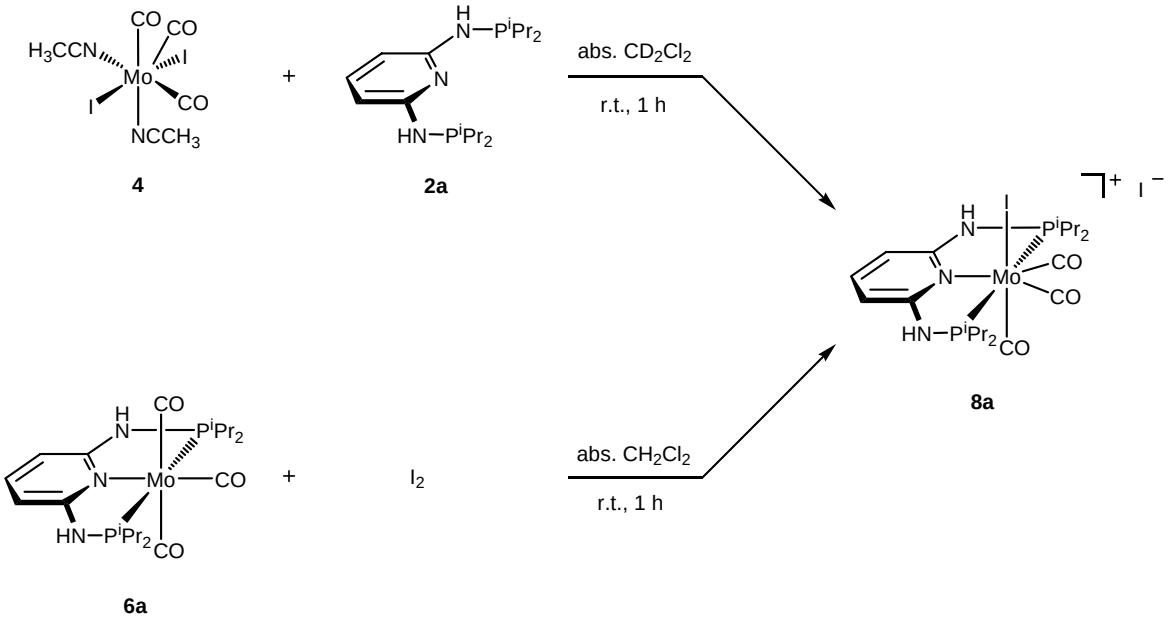

Figure 3.13 Two synthetic routes to [Mo(PNP-^{i}Pr)(CO)$_3$I]I (**8a**)

All products were characterized via ^{1}H and ^{31}P{^{1}H} NMR spectroscopy. Selected characteristic ^{1}H and ^{31}P{^{1}H} NMR resonances are given in Table 3.5.

Table 3.5 Comparison of selected ^{1}H and ^{31}P{^{1}H} NMR resonances of the halide complexes

	^{31}P{^{1}H} (δ [ppm], CD_2Cl_2, 20 °C)	**^{1}H (δ [ppm], CD_2Cl_2, 20 °C)**			
		py[4]	py[3,5]	N*H*	C*H*(CH$_3$)$_2$
8a	114.0	7.41 (1H)	7.21-7.03 (2H)	8.10 (2H)	3.87-3.65 (2H), 3.14-2.84 (2H)
8a'	112.8	7.55 (1H)	6.74-6.52 (2H)	6.29 (2H)	3.92-3.68 (2H), 2.98-2.70 (2H)
8b[1)]	113.8	7.62-7.43 (1H)[2)]	7.01 (1H), 6.88 (1H)	7.62-7.43 (1H)[2)], 7.98 (1H)	3.74-3.55 (1H), 3.05-2.84 (3H)
9a	117.0	7.45-7.30 (1H)	7.09 (1H), 6.73 (1H)	8.73 (1H), 8.30 (1H)	3.55-3.32 (1H), 2.98-2.61 (3H)

[1)] solvent: CD_3CN
[2)] overlap of py[4] and N*H* (1H)

The $^{31}P\{^{1}H\}$ NMR spectra exhibit resonances in the region around 115 ppm for all four complexes (compare Table 3.5). This shows only an minor dependence of the $^{31}P\{^{1}H\}$ NMR shifts on the nature of the halide and the counterion, respectively.

As shown in Table 3.5, in the ^{1}H NMR spectra a significant shift to the low field of the amino hydrogen atoms is observed (8.10 ppm for the amino hydrogen atoms in **8a** compared to 6.37 ppm in **6a**). This is a result of hydrogen bridges of the acidic amino hydrogen atoms.

The seven-coordinated geometry of this complexes results in a loss of symmetry. For **8a** and **8a'** this leads to different shifts for the CH groups "above" and "below" the plane of the ligand (see Figure 3.15), resulting in resonances at 3.87 – 3.65 and 3.14 – 2.84 ppm (**8a**) and 3.92 – 3.68 and 2.98 – 2.70 ppm (**8a'**). For the complexes **8b** and **9a** the resonances of the CH groups split in a 1:3 ratio and the resonances of the $py^{3,5}$ protons and the amino protons also split up.

Generally all resonances in the ^{1}H NMR spectra of the halide complexes **8** and **9** are shifted to the low field compared to the starting complex **6a**. The resonance of the py^{4} hydrogen atom is shifted from 7.16 (**6a**) to 7.41 ppm (**8a**) and the resonance of the $py^{3,5}$ hydrogen atoms is shifted from 6.13 (**6a**) to 7.21 – 7.03 ppm (**8a**) for example.

In addition all signals of the halide complexes were broadened. This is traced back to a fluxional behavior of seven-coordinated complexes in solution.

[Mo(PNP-^{i}Pr)$(CO)_3$Br]Br (**9a**) was crystallized from methylene chloride by diethyl ether diffusion. The crystal structure is given in Figure 3.14 along with selected crystallographic data (for more details see Chapter 5.7).

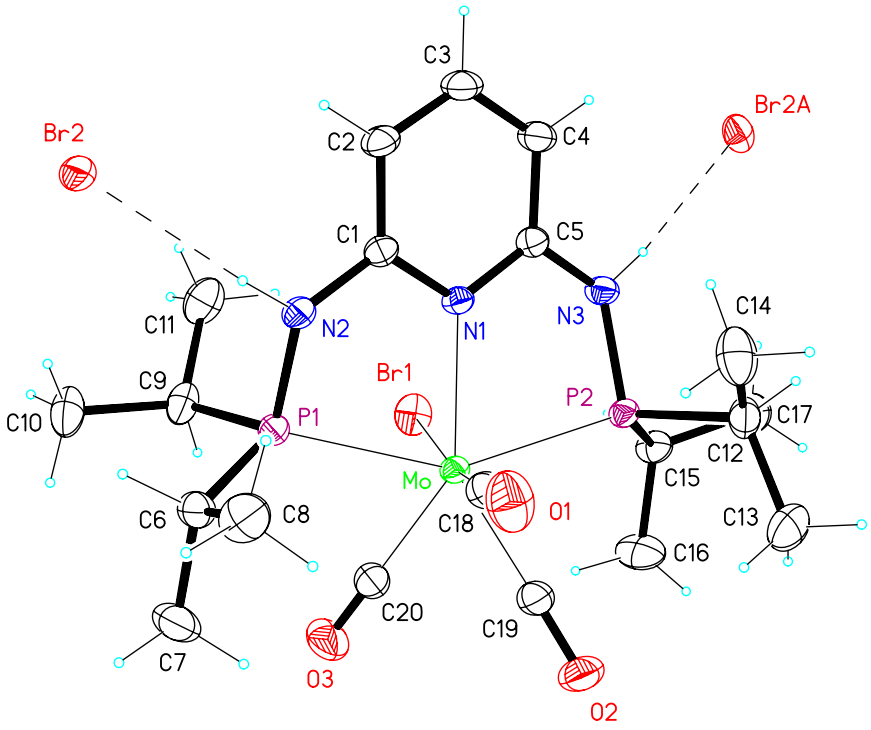

Figure 3.14 Structural view of [Mo(PNP-^{i}Pr)(CO)$_3$Br]Br (**9a**) showing 20 % thermal ellipsoids. Selected bond lengths (Å) and bond angles (°): Mo–C(18) 2.037(2), Mo–C(19) 1.979(2), Mo–C(20) 2.006(2), Mo–N(1) 2.2364(15), Mo–P(1) 2.5242(5), Mo–P(2) 2.5172(5), Mo–Br(1) 2.6713(3); P(1)–Mo–P(2) (150.796(17), N(1)–Mo–P(2) 75.67(4), N(1)–Mo–P(2) 75.37(4), N(1)–Mo–C(18) 85.95(7), N(1)–Mo–C(19) 144.18(8), N(1)–Mo–C(20) 144.17(7), N(1)–Mo–Br(1) 84.22.

The coordination geometry can be viewed as a distorted capped trigonal prism with N(1) capping the quadrilateral face. Figure 3.14 also shows the hydrogen bonds between the amino hydrogen atoms and the bromide counderions. The distortion is more apparent in the view shown in Figure 3.15. The phosphorus atoms are deviated from the plane of the aromatic ring. Therefore the two metallacycles are not longer in plane with the aromatic ring.

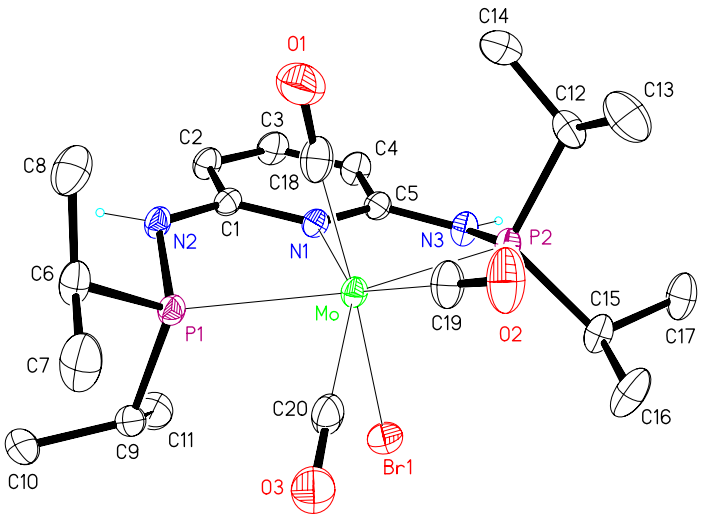

Figure 3.15 Alternative structural view of **9a** showing 20 % thermal ellipsoids (C-bound H atoms and Br^- omitted for clarity)

The complex Mo(PNP-^{i}Pr)(CO)$_3$ (**6a**) has shown its capability to undergo oxidative addition reactions with halogens. Based on these results preliminary studies were performed to investigate the reactivity towards other reagents.

As starting point reactions which were successfully performed starting from K[MoTp(CO)$_3$] were used, since this is also a molybdenum complex with three carbonyl ligands and a tridentate ligand. In contrast to the PNP complexes this complex is anionic and the Tp ligand is coordinated in a facial geometry.

3.5.2 Reaction with Methyl Iodide

K[MoTp(CO)$_3$] is known to react with alkyl halides to give the seven-coordinated complexes MoTp(CO)$_3$R (R = alkyl) (see Figure 3.16)[44].

[44] Trofimenko, S. *J. Am. Chem. Soc.* **1969**, *91*, 588.

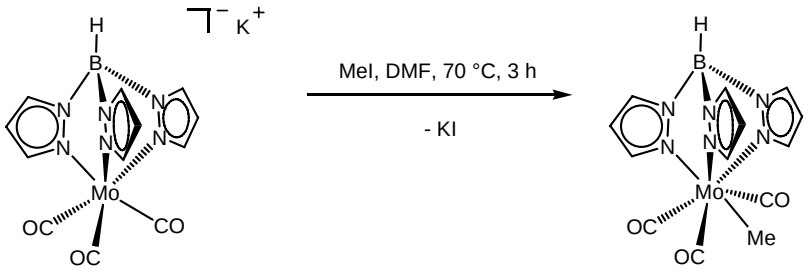

Figure 3.16 Reaction of K[MoTp(CO)$_3$] with methyl iodide

Therefore the reaction of the analogous neutral complex Mo(PNP-^{i}Pr)(CO)$_3$ (**6a**) with methyl iodide was studied. **6a** was reacted with methyl iodide in d$_3$-acetonitrile at room temperature and at 70 °C. The experiment was monitored via ^{1}H and ^{31}P{^{1}H} NMR spectroscopy but no reaction could be observed.

Surprisingly the neutral complex **6a** featuring a meridional coordinated PNP ligand does not undergo oxidative addition with alkyl halides.

3.5.3 Reaction with CF_3COOH

K[MoTp(CO)$_3$] reacts with acids under formation of hydride species (see Figure 3.17), e.g. with acetic acid in an aqueous solution.

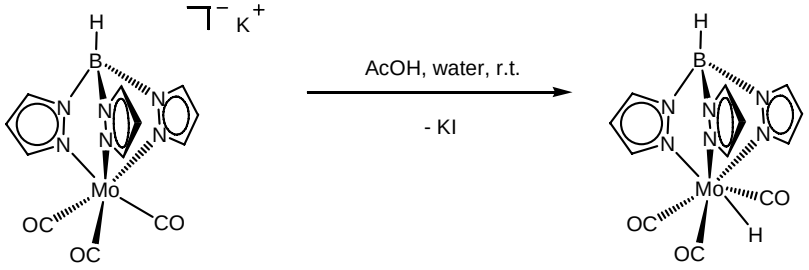

Figure 3.17 Reaction of K[MoTp(CO)$_3$] with acetic acid

Mo(PNP-^{i}Pr)(CO)$_3$ (**6a**) was reacted with trifluoroacetic acid in d$_3$-acetonitrile at room temperature. Effervescence was observed indicating the dissociation of one CO ligand. After 1 h complete conversion was observed via ^{1}H and ^{31}P{^{1}H} NMR spectroscopy. Isolation of the product failed due to degradation of the complex.

The ^{31}P{^{1}H} NMR spectrum did not exhibit new resonances, but in the ^{1}H NMR spectrum new resonances were observed. The most characteristic new resonances appear at -5.32, -5.46 and -5.61 ppm. The characteristic resonances of the ligand were also observed in the ^{1}H NMR spectrum, exhibiting resonances at 7.42 (py^4), 6.93 (N*H*), 6.38 (py^{3,5}), 2.78 – 2.52 (C*H*), and 1.47 – 1.11 (C*H*$_3$).

This indicates the formation of a new PNP hydride complex and is therefore a promising subject for further investigations.

3.5.4 Reaction with Allyl bromide

Oxidative addition of allyl bromide to K[MoTp(CO)$_3$] leads to the formation of MoTp(CO)$_2$(η^3-allyl) (see Figure 3.18).

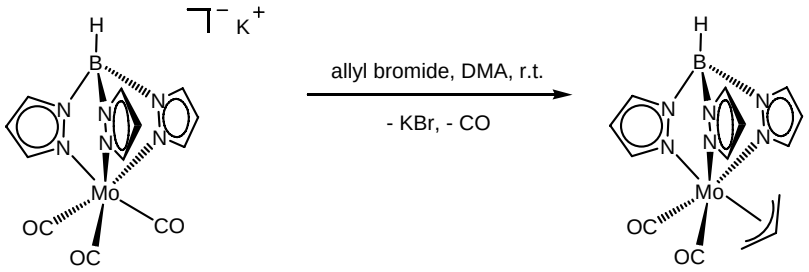

Figure 3.18 Reaction of K[MoTp(CO)$_3$] with allyl bromide

Analogously, **6a** was reacted with allyl bromide in d_3-acetonitrile at 70 °C for 18 h (see Figure 3.19). The reaction was monitored via $^{31}P\{^1H\}$ NMR spectroscopy and the spectrum showed the formation of a new phosphorus containing species with a resonance at about 125 ppm.

In another preliminary experiment the precursor Mo(η^3-allyl)(CO)$_2$(NCCH$_3$)$_2$Br (**5**) was reacted with PNP-^{i}Pr (**2a**) in acetonitrile at room temperature for 18 h (see Figure 3.19). The $^{31}P\{^1H\}$ NMR spectrum showed the formation of the same species.

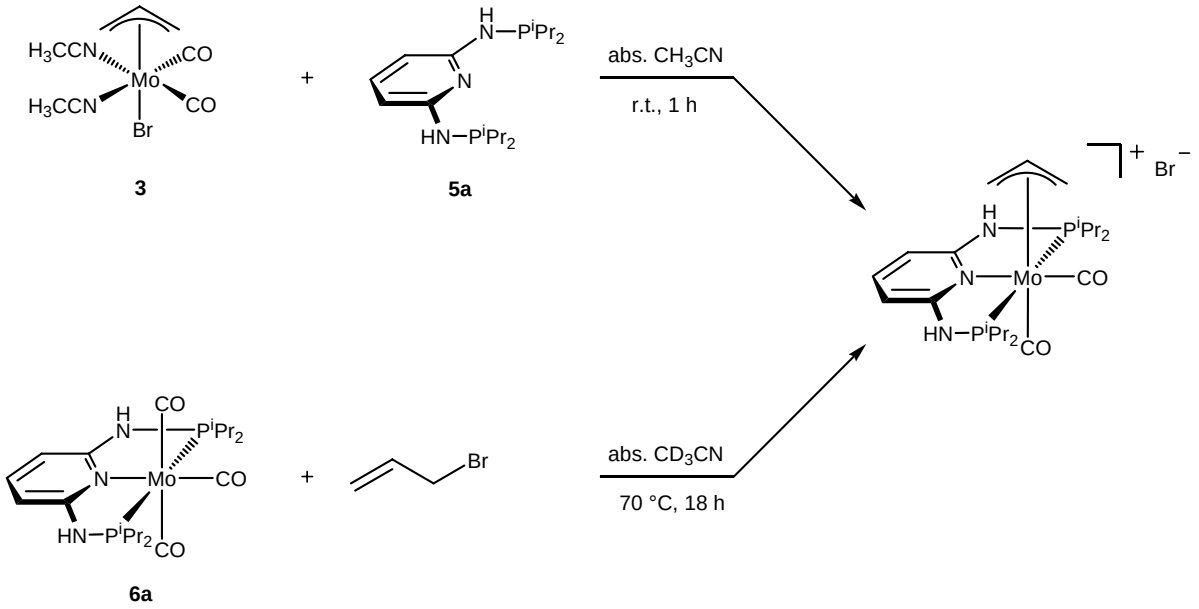

Figure 3.19 Reactions with allyl bromide

Figure 3.19 shows a plausible reaction leading to a η^3-allyl complex. These preliminary results show that **6a** is capable to undergo a reaction with allyl bromide. This interesting reaction will be subject of further investigation.

3.6 Reactions of [Mo(PNP-^{i}Pr)(CO)$_2$(NCCH$_3$)I]I

An immanent problem of the tricarbonyl complexes is their low reactivity because of the lack of labile ligands. PNP ligands are very strongly coordinated to the metal center as a result of their tridentate binding mode. The exchange of another CO ligand is also difficult, because they are also strongly bound as result of their ability to undergo π-backbonding. As the two neutral phosphorus donors and the pyridine nitrogen are better σ-donors than acetonitrile, the electron-density at the metal center is increased in comparison to the tricarbonyltris(acetonitrile) complexes precursor and the remaining three CO ligands are inert to substitution.

Since during the reaction of Mo(PNP-^{i}Pr)(CO)$_3$ (**6a**) with iodine in acetonitrile one CO ligand is replaced by another acetonitrile, a labile ligand is introduced into the system. Therefore [Mo(PNP-^{i}Pr)(CO)$_2$(NCCH$_3$)I]I (**8b**) was used as a starting material for further reactions.

3.6.1 Reaction with Methyl Iodide

Since it was shown that **6a** was not reactive enough to undergo a reaction with methyl iodide (see Chapter 3.5.2) an analogous reaction was carried out with **8b** as starting material.

8b and methyl iodide were reacted in d_2-methylene chloride at room temperature for 1 h. Since no reaction could be observed by monitoring the reaction via ^{1}H and ^{31}P{^{1}H} NMR spectroscopy, the reaction was warmed up to 40 °C for 18 h, but no reaction occurred.

Addition of zinc to the reaction mixture leads to the formation of Mo(PNP-^{i}Pr)(CO)$_2$(NCCH$_3$) (**11**) that was inert to the oxidative addition of methyl iodide under the reaction conditions.

This experiment showed that neither Mo(PNP-^{i}Pr)(CO)$_3$ (**6a**) nor [Mo(PNP-^{i}Pr)(CO)$_2$(NCCH$_3$)I]I (**8b**) or Mo(PNP-^{i}Pr)(CO)$_2$(NCCH$_3$) (**11**) were reactive enough to undergo oxidative addition of methyl iodide.

3.6.2 Reduction to Mo(PNP-^{i}Pr)(CO)$_2$(NCCH$_3$)

As via the reaction of Mo(PNP-^{i}Pr)(CO)$_3$ (**6a**) with iodine a Mo^{II} species with an additional labile acetonitrile ligand instead of one of the CO ligands was obtained, it was of interest to see if analogous Mo^0 complexes could also be prepared.

Therefore, [Mo(PNP-^{i}Pr)(CO)$_2$(NCCH$_3$)I]I (**8b**) was reacted for 1 h with 2 equiv. of zinc to remove both iodine atoms and to obtain Mo(PNP-^{i}Pr)(CO)$_2$(NCCH$_3$) (**11**). The reaction was carried out in d_3-acetonitrile and d_2-methylene chloride at room temperature (see Figure 3.20). The product could not be isolated and purified due to its instability.

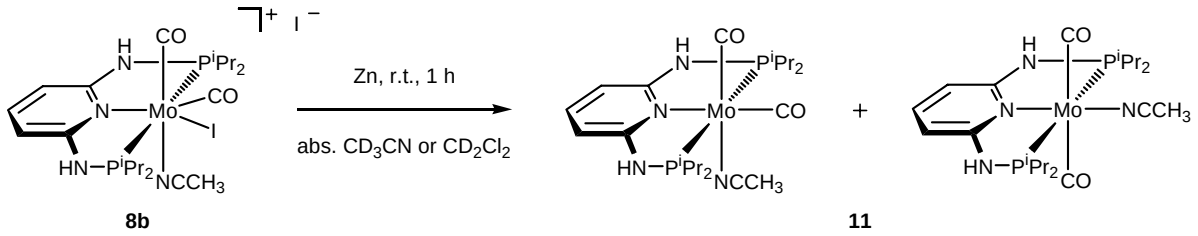

Figure 3.20 Preparation of Mo(PNP-iPr)(CO)$_2$(NCCH$_3$) (**11**)

The reaction was monitored via ^{1}H and ^{31}P{^{1}H} NMR spectroscopy. The ^{31}P{^{1}H} NMR spectrum exhibits two resonances at 123.4 and 123.1 ppm respectively. A plausible explanation is the formation of two isomers (see Figure 3.20). The ^{1}H NMR spectrum exhibits the characteristic pattern for the pyridine and amine hydrogen atoms of the PNP-^{i}Pr ligand without differentiation of the two isomers. The signals for the C*H*(CH$_3$)$_2$ hydrogen atoms split up into two signals at 2.79-2.61 and 2.57-2.40 ppm, respectively, representing 2 hydrogen atoms each. The equality of the integrals of the two resonances for the different C*H*(CH$_3$)$_2$ groups corresponds to a 1:1 ratio of the two isomers, which was also observed in the ^{31}P{^{1}H} NMR spectrum. When the reaction was carried out in d_2-methylene chloride, also the resonance of the acetonitrile ligand at 2.01 ppm could also be observed, but the other signals were hard to detect because of the low solubility of **11** in this solvent.

3.7 Self-Exchange Atom Transfer Experiments

The mechanism of electron transfer reactions between transition metal complexes has been widely studied. The mechanisms of electron transfer reactions are split into inner-sphere and outer-sphere electron transfer reactions. During an inner-sphere transfer reaction no ligand is exchanged between the two reacting complexes whereas during outer-sphere transfer reactions a least one ligand is transferred from one metal center to the other. Therefore outer-sphere electron transfer reactions are also called atom transfer or self-exchange reactions. Nearly every electron transfer reaction in solution involves atom transfer and the transferred atoms are often halides. Based on these facts it was tried to find out whether pincer complexes are also able to undergo self-exchange atom transfer reactions.

As starting point for this experiment the work of Creutz and coworkers about self-exchange atom transfer reactions[45] was chosen, because they also worked with group 6 transition metal halocarbonyl complexes, but instead of pincer complexes they studied Cp complexes. In contrast to PNP ligands, Cp ligands can be considered as facial coordinating ligands. Another difference between the two systems is the negative charge of the Cp ligand in contrast to the neutral PNP ligand.

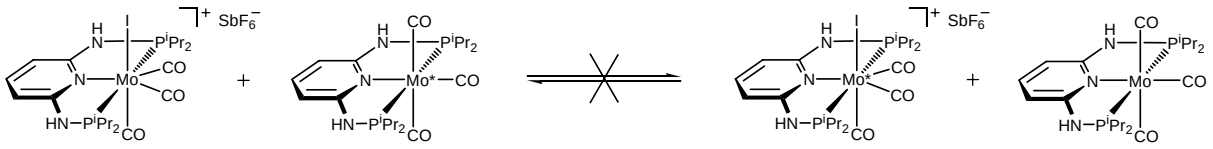

Figure 3.21 Self-exchange atom transfer experiment

Mo(PNP-^{i}Pr)(CO)$_3$ (**6a**) and [Mo(PNP-^{i}Pr)(CO)$_3$I](SbF$_6$) (**8a'**) were dissolved CD_2Cl_2 in a NMR tube. ^{1}H and ^{31}P{^{1}H} NMR spectra were recorded and determined if the signals had broadened, which would indicate a self-exchange atom transfer reaction between the two complexes. Neither at room temperature nor at elevated temperatures (40 °C) broadening of the signals could be observed. Since for the Cp systems an exchange could be observed down to – 20 °C it can be assumed that the pincer systems do not undergo self-exchange atom transfer reactions.

3.8 Reaction with Alkynes

Transition metal complexes with metal-carbon double or triple bonds such as carbenes, carbynes, vinylidenes, or allenylidenes are of great interest in various fields of organometallic and synthetic organic chemistry. Metal carbenes for example are widely used for olefin metathesis (see Chapter 2.3). Therefore in this work it was attempted to synthesize products with molybdenum carbon multiple bonds. One approach to that topic is the substitution of a labile ligand against an alkyne which in a first step forms a π-complex but then quickly rearranges to a vinylidene (see Figure 3.22)[46].

[45] Schwarz, C. L.; Bullock, R. M.; Creutz, C. *J. Am. Chem. Soc.* **1991**, *113*, 1225.
[46] (a) Birdwhistell, K. R.; Nieter Burgmayer, S. J.; Templeton, J. L. *J. Am. Chem. Soc.* **1983**, *105*, 7789. (b) Birdwhistell, K. R.; Tonker, T. L.; Templeton, J. L. *J. Am. Chem. Soc.* **1985**, *107*, 4474. (c) Birdwhistell, K. R.; Tonker, T. L.; Templeton, J. L. *J. Am. Chem. Soc.* **1987**, *109*, 1401.

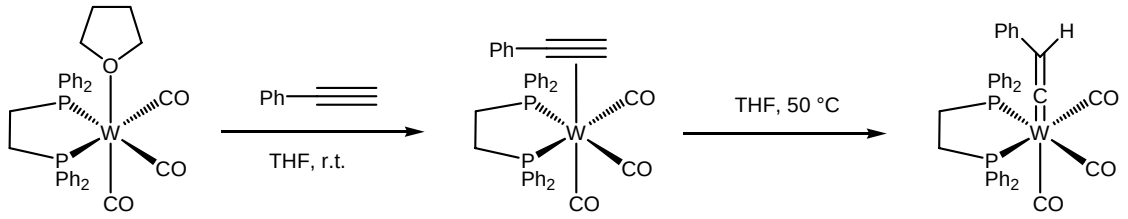

Figure 3.22 Synthesis of a tungsten vinylidene complex

Starting point for the experiments in this work were the complexes [Mo(PNP-^{i}Pr)(CO)$_2$(NCCH$_3$)I]I (**8b**) and Mo(PNP-^{i}Pr)(CO)$_2$(NCCH$_3$) (**11**) because of their labile acetonitrile ligands. As alkynes 2-propyn-1-ol, 3-butin-1-ol, methyl propiolate, phenylacetylene, p-tolylacetylene and the more reactive Li-phenylacetylide were tested (see Figure 3.23).

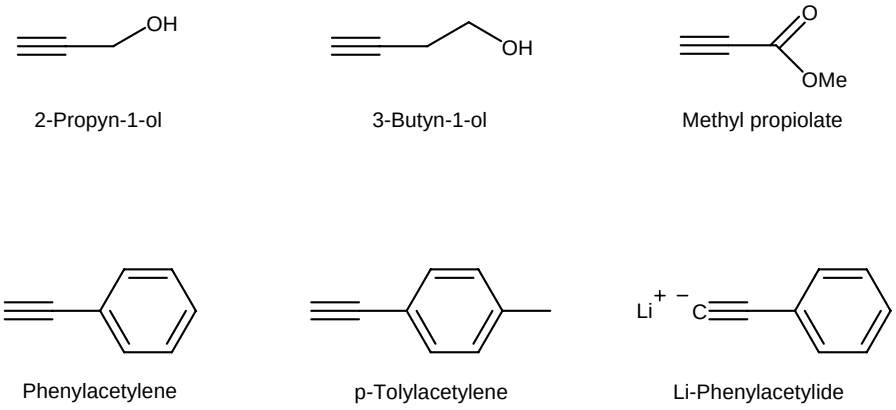

Figure 3.23 Used alkynes

It was tried to react **8b** and **11** with the alkynes and also to reduce **8b** to **11** in the presence of alkynes. All these attempts did not lead to the desired vinylidene products. Due to the great interest of these compounds the formation of vinylidenes will be further investigated and alternative synthetic routes will be studied.

4 Summary and Outlook

In the course of this work the modular approach to new PNP pincer ligands was successfully used to prepare new ligands and molybdenum and tungsten complexes thereof.

The chlorophosphites BIPOL-PCl (**1a**) and TAR^{Me}-PCl (**1b**) were prepared as building blocks for the PNP ligands in a reaction between PCl_3 and the respective diols in 87 and 80 % yield. The ligands PNP-^{i}Pr (**2a**) and PNP-^{t}Bu (**2b**) based on chlorophosphines, and PNP-BIPOL (**2c**) and PNP-TAR^{Me} (**2d**) based on the chlorophosphites **1a** and **1b** were synthesized in 54 – 74 % yield. The PNP pincer ligands were prepared in condensation reactions of 2,6-diaminopyridine and the corresponding chlorophosphines and chlorophosphites.

These ligands were reacted with $Mo(CO)_3(NCCH_3)_3$ (**3a**) and $W(CO)_3(NCCH_3)$ (**3a'**) to give the complexes Mo(PNP-^{i}Pr)$(CO)_3$ (**6a**), Mo(PNP-^{t}Bu)$(CO)_3$ (**6b**) and W(PNP-^{i}Pr)$(CO)_3$ (**6a'**) in 62, 15, and 6 % yield. The complexation with the ligands **2c** and **2d** failed.

Starting from the alternative precursor $Mo(CO)_4(NCCH_3)_2$ (**3b**) the new complexes Mo(PN(P)-^{i}Pr)$(CO)_4$ (**7a**) and Mo(PN(P)-^{t}Bu)$(CO)_4$ (**7b**) were prepared in 58 and 27 % yield. In these complexes the pincer ligands only coordinate via the pyridine nitrogen and one of the phosphorus atoms whereas the second phosphorus atom remains non-coordinating.

Starting from **6a** the reactivity of the molybdenum pincer complexes was studied. The complexes [Mo(PNP-^{i}Pr)$(CO)_3$I]I (**8a**) and [Mo(PNP-^{i}Pr)$(CO)_3$Br]Br (**9a**) were prepared in quantitative yield by reacting **6a** in methylene chloride with iodine and bromine, respectively. The preparation of **8a** was also carried out via an alternative route starting from $MoI_2(CO)_3(NCCH_3)_2$ (**4**) and **2a**. A single crystal structure **9a** was determined. Reacting **6a** with iodine in acetonitrile afforded [Mo(PNP-^{i}Pr)$(CO)_2(NCCH_3)$I]I (**8b**) in quantitative yield. This opened access to new complexes with a labile acetonitrile ligand instead of one CO ligand. Via the reduction of **8b** with zinc the complex Mo(PNP-^{i}Pr)$(CO)_2(NCCH_3)$ (**11**) was obtained. These reactions showed the tendency of the complexes to perform oxidative addition of halogens.

Preliminary studies have been carried out to study the reactivity towards other reagents like allyl bromide or acids. **2a** was reacted with CF_3COOH giving a new pincer hydride species. Both reactions were only preliminary studies so far and the products are not fully characterized yet. These reactions will be further investigated and the products will be characterized in due course.

8b and **11** were used as starting materials for attempts to form vinylidene complexes via a reaction with alkynes. Unfortunately all attempts failed so far, but alternative methods will be further investigated.

Finally it was studied if the complexes **6a** and [Mo(PNP-^{i}Pr)$(CO)_3$I](SbF_6) (**8a'**) were able to undergo a self-exchange atom transfer reaction, which was not the case.

Within the scope of this work it was shown that the modular PNP pincer ligand system based on 2,6-diaminopyridine is capable of preparing a new class of molybdenum and tungsten pincer complexes. These complexes are reactive in oxidative addition reactions with halogens and related compounds.

Preliminary studies showed that the new molybdenum and tungsten complexes open a promising field for further investigations.

Since the reactivity studies were carried out with Mo(PNP-^{i}Pr)(CO)$_3$ (**6a**) as model complex, they have to be tested with the other ligands too, to study the influences of the ligands on the reactivity of the metal center. The same has to be done for tungsten complexes with various ligands.

The complexes [Mo(PNP-^{i}Pr)(CO)$_2$(NCCH$_3$)I]I (**8b**) and Mo(PNP-^{i}Pr)(CO)$_2$(NCCH$_3$) (**11**) represent an interesting alternative for the reaction with less reactive reagents because of their labile acetonitrile ligand. Although all attempts to form molybdenum vinylidene pincer complexes failed so far, this is a field of great interest in terms of potential catalytic applications.

Another approach to the synthesis of new molybdenum and tungsten pincer complexes is to use of alternative metal precursors as starting materials, for example MoCl$_5$[47]. This will lead to novel molybdenum pincer complexes with alternative co-ligands.

Another interesting task would be the preparation of molybdenum and tungsten PCP complexes based on ligands analogous to the ligands presented in this work.

[47] Dilworth, J. R.; Richards, R. L.; Chen, G. J.-J.; McDonald, J. W. *Inorg. Synth.* **1990**, *28*, 33.

5 Experimental Section

5.1 General

All manipulations were performed under an inert atmosphere of argon using standard Schlenk techniques. The starting materials chloro-diisopropylphosphine, chloro-di-*tert*-butylphosphine, 2,2'-biphenol, phosphorus trichloride, *N*-methylpyrrolidone and molybdenumhexacarbonyl were purchased from Aldrich and used without further purification. 2,6-diaminopyridine was purified by hot filtration from methylene chloride over active carbon. Tungstenhexacarbonyl was purified via sublimation at 100 °C and atmospheric pressure. The solvents were purified according to standard procedures[48]. The deuterated solvents were purchased from Aldrich and Eurisotop, degassed, and dried over 4 Å molecular sieves.

^{1}H, $^{13}C\{^{1}H\}$, and $^{31}P\{^{1}H\}$ NMR spectra were recorded on a Bruker AVANCE-250 spectrometer, working at 250.13, 62.86, and 101.26 MHz, respectively. The spectra were referenced to $SiMe_4$ and H_3PO_4 (85 %), respectively.

The infrared spectra were collected on a Bruker TENSOR 27 spectrometer using a ZnSe ATR unit.

The X-ray data were collected on a Bruker Smart CCD area detector diffractometer using graphite-monochromated Mo K_α radiation (λ = 0.71073 Å) and 0.3 ° ω-scan frames covering complete spheres of the reciprocal space. Corrections for absorptions, $\lambda/2$ effects, and crystal decay were applied[49]. The structures were solved by direct methods using the program SHELXS97[50]. Structure refinement on F^2 was carried out with the program SHELXL97. All non-hydrogen atoms were refined anisotropically. Hydrogen atoms were inserted in idealized positions and were refined riding on the atoms to which they were bonded, using AFIX 137 orientation refinement to acetonitrile CH_3 groups. Badly disordered solvents were squeezed with the program PLATON prior to final refinement[51].

---

[48] Perrin, D. D.; Armarego, W. L. F. *Purification of Laboratory Chemicals*, 3rd ed., Pergamon, New York, **1988**.
[49] Bruker programs: *SMART*, version 5.054; *SAINT*, version 6.2.9; *SADABS*, version 2.10; *XPREP*, version 5.1; *SHELXTL*, version 5.1; Bruker AXS Inc.: Madison, WI, 2001.
[50] Sheldrick, G. M. *SHELX97*: Program System for Crystal Structure Determination; University of Göttingen: Göttingen, Germany, **1997**.
[51] Spek, A. L. *PLATON: A Multipurpose Crystallographic Tool*; University of Utrecht: Utrecht, The Netherlands, **2004**.

5.2 Preparation of the Ligand Building Blocks

5.2.1 Preparation of 2-Chlorodibenzo[*d*,*f*]-1,3,2-dioxaphosphepine (BIPOL-PCl) (1a)

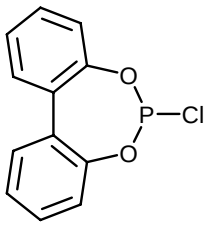

10.00 g	(53.71 mmol)	2,2'-biphenol
25.81 g	(188.00 mmol)	phosphorus trichloride
0.532 g	(5.367 mmol)	*N*-methylpyrrolidone

A 100 mL three-necked round-bottom flask equipped with a septum, a reflux-condenser and a connection to the Schlenk line was loaded with 2,2'-biphenol and cooled to 0 °C. *N*-methylpyrrolidone and phosphorus trichloride were added and the mixture was stirred for 3 h at 80 °C. The excess of phosphorus trichloride was removed under vacuum. Bulb-to-bulb distillation (200 °C / 10^{-4} mbar) of the crude product gave a bright yellow oil which crystallized in the refrigerator.

Yield:	11.75 g (87 %)	white microcrystalline solid
$C_{12}H_8ClO_2P$		MW = 250.62 g mol^{-1}

^{1}H NMR(δ [ppm], $CDCl_3$, 20 °C): 7.58-7.22 (m, 8H).

$^{31}P\{^{1}H\}$ NMR(δ [ppm], $CDCl_3$, 20 °C): 179.6.

5.2.2 Preparation of 2-Chloro-(4*R*,5*R*)-dicarbomethoxy-1,3,2-dioxaphospholane (TAR^{Me}-PCl) (1b)

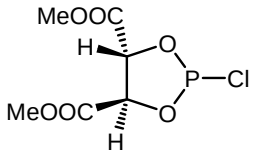

7.66 g	(43.00 mmol)	L-(+)-methyl tartrate
20.74 g	(151.00 mmol)	phosphorus trichloride
0.532 g	(0.43 mmol)	*N*-methylpyrrolidone

A 100 mL three-necked round-bottom flask equipped with a septum, a reflux-condenser and a connection to the Schlenk line was loaded with L-(+)-methyl tartrate and cooled to 0 °C. *N*-methylpyrrolidone and phosphorus trichloride were added and effervescence could be observed immediately. The mixture was warmed to 60 °C after effervescence stopped and stirred at this temperature for 2 h. The excess of phosphorus trichloride was removed under vacuum. Bulb-to-bulb distillation (150 °C / 10^{-4} mbar) of the crude product gave a colorless oil.

Yield:	8.36 g (80 %)	colorless oil
$C_6H_8ClO_6P$		MW = 242.55 g mol^{-1}

^{1}H NMR(δ [ppm], $CDCl_3$, 20 °C): 5.57 (d, *J* = 6.2 Hz, 1H, C*H*), 4.79 (dd, *J* = 6.2 Hz, J_{PH} = 9.8 Hz, 1H, C*H*), 3.33 (s, 3H, CH_3), 3.24 (s, 3H, CH_3)

^{31}P{^{1}H} NMR(δ [ppm], $CDCl_3$, 20 °C): 174.6.

5.3 Preparation of the Ligands

5.3.1 Preparation of *N,N'*-Bis(diisopropylphosphino)-2,6-diaminopyridine (PNP-^{i}Pr) (2a)

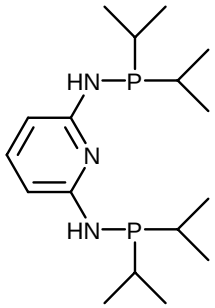

1.003 g	(9.191 mmol)	2,6-diaminopyridine
2.800 g	(18.347 mmol)	chloro-diisopropylphosphine
1.855 g	(18.332 mmol)	triethylamine
25 mL		abs. toluene

A Schlenk-flask was loaded with 2,6-diaminopyridine and 25 mL of abs. toluene were added. The mixture was cooled to 0 °C and triethylamine was added. After 15 min. of stirring and cooling, chloro-diisopropylphosphine was added. The reaction-mixture was heated to 80 °C, stirred for 18 h at this temperature, and afterwards cooled to room temperature. The ammonium salt was filtered off, the solvent was evaporated and the product dried under high vacuum.

Yield:	3.357g (97 %)	white solid
$C_{17}H_{33}N_3P_2$		FW = 341.42 g·mol^{-1}

^{1}H NMR(δ [ppm], $CDCl_3$, 20 °C): 7.23 (t, *J* = 7.9 Hz, 1H, py^{4}), 6.42 (dd, *J* = 7.9 Hz, *J* = 2.3 Hz, 2H, py^{3,5}), 4.29 (d, *J* = 11.2 Hz, 2H, N*H*), 1.78-1.67 (m, 4H, C*H*$(CH_3)_2$), 1.08-0.99 (m, 24H, CH(C*H*$_3)_2$).

^{13}C{^{1}H} NMR(δ [ppm], $CDCl_3$, 20 °C): 159.5 (d, *J* = 20.3 Hz, py^{2,6}), 139.1 (py^{4}), 98.1 (d, *J* = 18.4 Hz, py^{3,5}), 26.3 (d, *J* = 10.7 Hz, *C*H$(CH_3)_2$), 18.6 (d, *J* = 19.6 Hz, CH(*C*H$_3)_2$), 17.1 (d, *J* = 7.7 Hz, CH(*C*H$_3)_2$).

^{31}P{^{1}H} NMR(δ [ppm], $CDCl_3$, 20 °C): 49.0.

5.3.2 Preparation of *N,N'*-Bis(di-*tert*-butylphosphino)-2,6-diaminopyridine (PNP-^{t}Bu) (2b)

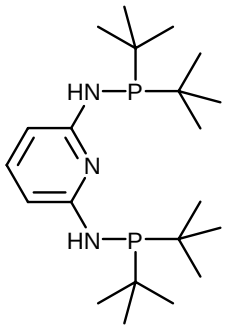

1.205 g	(11.042 mmol)	2,6-diaminopyridine
3.994 g	(22.108 mmol)	chloro-di-*tert*-butylphosphine
2.236 g	(22.097 mmol)	triethylamine
1.415 g	(22.089 mmol)	*n*-butyl lithium (2.3 M solution in *n*-hexane)
25 mL		abs. toluene

A Schlenk-flask was loaded with 2,6-diaminopyridine and triethylamine and 25 mL of abs. toluene were added. The mixture was cooled to -80 °C and *n*-butyl lithium was added. After 30 min. of stirring and cooling the reaction mixture was warmed to room temperature and stirred for 2 h. Chloro-di-*tert*-butylphosphine was added and the reaction mixture was stirred at 80 °C for 18 h. After cooling to room temperature the solution was filtered and the solvent was evaporated. The crude product was recrystallized from toluene/n-hexane (1:1) and dried under high vacuum.

Yield:	2.381 g (54 %)	brown solid
$C_{21}H_{41}N_3P_2$		FW = 397.52 g·mol^{-1}

^{1}H NMR(δ [ppm], $CDCl_3$, 20 °C): 7.25 (t, *J* = 7.7 Hz, 1H, py^{4}), 6.48 (dd, *J* = 7.7 Hz, *J* = 2.5 Hz, 2H, py^{3,5}), 4.64 (d, *J* = 11.2 Hz, 2H, N*H*), 1.22-1.15 (m, 36H, C(C*H*$_3$)$_3$).

^{13}C{^{1}H} NMR(δ [ppm], $CDCl_3$, 20 °C): 155.1 (py^{2,6}), 138.7 (py^{4}), 98.2 (d, *J* = 18.5 Hz, py^{3,5}), 29.4 (d, *J* = 13.9 Hz, *C*(CH$_3$)$_3$), 27.8 (d, *J* = 15.0 Hz, C(*C*H$_3$)$_3$).

^{31}P{^{1}H} NMR(δ [ppm], $CDCl_3$, 20 °C): 60.2.

5.3.3 Preparation of *N,N'*-Bis(dibenzo[*d,f*]-1,3,2-dioxaphosphepine)-2,6-diaminopyridine (PNP-BIPOL) (2c)

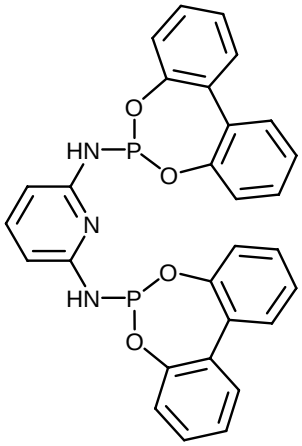

0.435 g	(3.986 mmol)	2,6-diaminopyridine
1.996 g	(7.964 mmol)	2-chlorodibenzo[*d,f*][1,3,3]dioxaphosphepine (**1a**)
0.813 g	(8.034 mmol)	triethylamine
30 mL		abs. toluene

A Schlenk-flask was loaded with 2,6-diaminopyridine and 25 mL of abs. toluene were added. The mixture was cooled to 0 °C and triethylamine was added. After 15 min. of stirring and cooling, 2-chlorodibenzo[*d,f*]-1,3,2-dioxaphosphepine (**1a**) and further 5 mL of abs. toluene were added. The reaction-mixture was heated to 80 °C and stirred at this temperature for 18 h. After cooling to room temperature the solution was filtered and the solvent was evaporated. The crude product was recrystallized from toluene/*n*-hexane (1:1) and dried under high vacuum.

Yield:	1.803 g (84 %)	white solid
$C_{29}H_{21}N_3O_4P_2$		FW = 537.45 g·mol^{-1}

^{1}H NMR(δ [ppm], $CDCl_3$, 20 °C): 7.50-7.15 (m, 9H, Ph^{3,5} and py^{4}), 6.40 (d, *J* = 7.8 Hz, 4H, Ph^{4}), 6.11 (dd, *J* = 31.6 Hz, *J* = 7.8 Hz, 4H, Ph^{6}), 5.89 (d, *J* = 7.8 Hz, 2H, py^{3,5}), 4.32 (bs, 2H, N*H*).

^{13}C{^{1}H} NMR(δ [ppm], $CDCl_3$, 20 °C): 154.2 (d, *J* = 17.3 Hz, py^{2,6}), 149.5 (d, *J* = 3.8 Hz, Ph), 140.0 (py^{4}), 131.6 (d, *J* = 3.1, Ph), 129.8 (Ph), 129.2 (Ph), 125.3 (Ph), 122.3 (Ph), 101.5 (d, *J* = 12.3 Hz, py^{3,5}).

^{31}P{^{1}H} NMR(δ [ppm], $CDCl_3$, 20 °C): 147.2.

5.3.4 Preparation of *N*,*N*'-Bis((4*R*,5*R*)-dicarbomethoxy-1,3,2-dioxaphospholane)-2,6-diaminopyridine (PNP-TAR^{Me}) (2d)

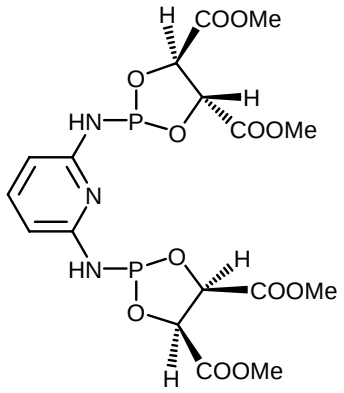

0.410 g	(3.757 mmol)	2,6-diaminopyridine
1.824 g	(7.520 mmol)	2-Chloro-(4*R*,5*R*)-dicarbomethoxy-1,3,2-dioxaphospholane (**1b**)
0.813 g	(8.034 mmol)	triethylamine
25 mL		abs. toluene

A Schlenk-flask was loaded with 2,6-diaminopyridine and 25 mL of abs. toluene were added. The mixture was cooled to 0 °C and triethylamine was added. After 15 min. of stirring and cooling, 2-chloro-(4*R*,5*R*)-dicarbomethoxy-1,3,2-dioxaphospholane (**1b**) were added. The reaction-mixture was heated to 80 °C and stirred at this temperature for 18 h. After cooling to room temperature the solution was filtered and the solvent was evaporated. The crude product was recrystallized from toluene/*n*-hexane (1:1) and dried under high vacuum.

Yield:	1.456 g (74 %)	white solid
$C_{17}H_{21}N_3O_{12}P_2$		FW = 521.32 g·mol^{-1}

^{1}H NMR(δ [ppm], $CDCl_3$, 20 °C): 7.30 (t, *J* = 7.9 Hz, 1H, py^{4}), 6.45 (s, 2H, N*H*), 6.28 (d, *J* = 7.9 Hz, 2H, py^{3,5}), 5.06-5.03 (m, 2H, C*H*), 4.81-4.75 (m, 2H, C*H*), 3.83 (s, 12H, CH_3).

^{13}C{^{1}H} NMR(δ [ppm], $CDCl_3$, 20 °C): 171.3 (*C*O), 169.0 (*C*O), 153.8 (d, *J* = 14.9 Hz, py^{2,6}), 139.7 (py^{4}), 101.9 (d, *J* = 10.3 Hz, py^{3,5}), 77.6 (*C*H), 77.1 (*C*H), 76.7 (t, *J* = 10.1 Hz, *C*H_3), .53.2 (t, *J* = 15.5 Hz, *C*H_3).

^{31}P{^{1}H} NMR(δ [ppm], $CDCl_3$, 20 °C): 142.9.

5.4 Preparation of the Molybdenum and Tungsten Precursors

5.4.1 Preparation of $Mo(CO)_3(NCCH_3)_3$ (3a)

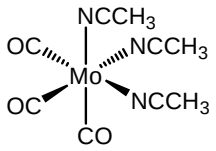

0.264 g	(1.000 mmol)	molybdenumhexacarbonyl
10 mL		abs. acetonitrile

A Schlenk-flask was loaded with molybdenumhexacarbonyl and 10 mL of abs. acetonitrile were added. The mixture was heated to 85 °C. After 4 h of refluxing the bright yellow solution was cooled to room temperature. The product was not isolated.

Yield:	product not isolated
$C_9H_9MoN_3O_3$	FW = 303.13 g·mol^{-1}

5.4.2 Preparation of $Mo(CO)_4(NCCH_3)_2$ (3b)

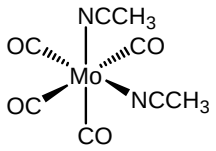

0.264 g	(1.000 mmol)	molybdenumhexacarbonyl
10 mL		abs. acetonitrile

A Schlenk-flask was loaded with molybdenumhexacarbonyl and 10 mL of abs. acetonitrile were added. The mixture was heated to 70 °C. After 3 h the bright yellow solution was cooled to room temperature. The product was not isolated.

Yield:	product not isolated
$C_8H_6MoN_2O_4$	FW = 290.09 g·mol^{-1}

5.4.3 Preparation of $W(CO)_3(NCCH_3)_3$ (3a')

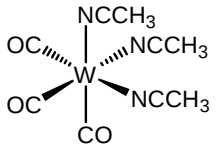

0.352 g	(1.000 mmol)	tungstenhexacarbonyl
15 mL		abs. acetonitrile

A Schlenk-flask was loaded with tungstenhexacarbonyl and 15 mL of abs. acetonitrile were added. The mixture was heated to 85 °C and refluxed at this temperature for 7 d. The solution was degassed during the refluxing several times to remove the released CO by evacuating the flask and refilling it with argon. The product was not isolated but reacted *in situ*.

Yield:	product not isolated
$C_9H_9N_3O_3W$	FW = 391.04 g·mol^{-1}

5.4.4 Preparation of $MoI_2(CO)_3(NCCH_3)_2$ (4)

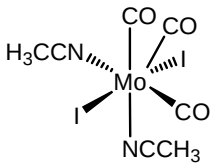

0.315 g	(1.193 mmol)	molybdenumhexacarbonyl
0.305 g	(1.202 mmol)	iodine
17 mL		abs. acetonitrile

A Schlenk-flask was loaded with molybdenumhexacarbonyl and 10 mL of abs. acetonitrile were added. The mixture was heated to 85 °C. Sublimed molybdenumhexacarbonyl was washed into the reaction mixture with 7 mL of abs. acetonitrile. After 18 h of refluxing the bright yellow solution was

cooled to 0 °C whereupon a white solid precipitated. Iodine was added, the color of the solution changed to dark red and effervescence could be observed. The solution was warmed to room temperature and the system was degassed by evacuating and refilling with argon several times. After 1 h the solvent was evaporated and a red-brown solid was obtained.

Yield:	0.554 g (90 %)	red-brown solid
$C_7H_6I_2MoN_2O_2$		FW = 515.89 g·mol^{-1}

IR (ATR, cm^{-1}): 2304 (m, $\nu_{C\equiv N}$), 2277 (m, $\nu_{C\equiv N}$), 2015 (s, $\nu_{C\equiv O}$), not observed (Shoulder of Peak at 2015) ($\nu_{C\equiv O}$), 1918 (s, $\nu_{C\equiv O}$).

5.4.5 Preparation of Mo(η^3-allyl)(CO)$_2$(NCCH$_3$)$_2$Br (5)

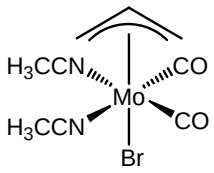

0.500 g	(1.894 mmol)	molybdenumhexacarbonyl
0.231 g	(1.907 mmol)	allyl bromide
20 mL		abs. acetonitrile

A Schlenk-flask was loaded with molybdenumhexacarbonyl and 20 mL of abs. acetonitrile were added. The mixture was heated to 85 °C and refluxed for 4 h. The solution was cooled to 0 °C and allyl bromide was added, whereupon an orange precipitate formed. The solution was warmed to room temperature and the system was stirred for 6 days until no more effervescence could be observed when the flask was purged with argon. The product was not isolated.

Yield:	product not isolated
$C_9H_{11}BrMoN_2O_2$	FW = 355.04 g·mol^{-1}

5.5 Preparation of the Pincer Complexes

5.5.1 Preparation of Mo(PNP-^{i}Pr)(CO)$_3$ (6a)

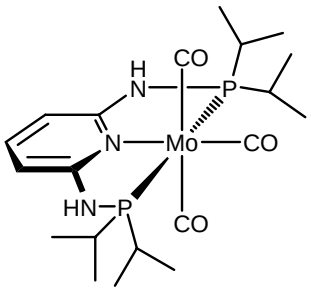

0.776 g	(2.939 mmol)	molybdenumhexacarbonyl
1.003 g	(2.938 mmol)	*N,N'*-bis(diisopropylphosphino)-2,6-diaminopyridine (**5a**)
23 mL		abs. acetonitrile

A Schlenk-flask was loaded with molybdenumhexacarbonyl and 10 mL of abs. acetonitrile were added. The mixture was heated to 85 °C. Sublimed molybdenumhexacarbonyl was washed into the reaction mixture with 5 mL of abs. acetonitrile. After 4 h of refluxing the bright yellow solution was cooled to room temperature and *N,N'*-bis(diisopropylphosphino)-2,6-diaminopyridine and further 8 mL of abs. acetonitrile were added. The solution was stirred at room temperature for 18 h. The solvent was evaporated under vacuum and the crude product was purified via column chromatography (neutral Al_2O_3, eluent: methylene chloride).

Yield:	0.957 g (62 %)	yellow solid
$C_{20}H_{33}MoN_3O_3P_2$		FW = 521.39 g·mol^{-1}

^{1}H NMR(δ [ppm], CD_3CN, 20 °C): 7.16 (t, *J* = 7.9 Hz, 1H, py^{4}), 6.37 (bs, 2H, N*H*), 6.13 (d, *J* = 7.9 Hz, 2H, py^{3,5}), 2.45-2.18 (m, 4H, C*H*(CH$_3$)$_2$), 1.33-1.03 (m, 24H, CH(C*H*$_3$)$_2$).

^{13}C{^{1}H} NMR(δ [ppm], CD_3CN, 20 °C): 231.4 (t, *J* = 5.8 Hz, *C*O), 216.9 (t, *J* = 10.4 Hz, *C*O), 161.0 (t, *J* = 7.8 Hz, py^{2,6}), 137.7 (py^{4}), 97.1 (t, *J* = 3.1 Hz, py^{3,5}), 31.6 (t, *J* = 10.4 Hz, *C*H(CH$_3$)$_2$), 18.1 (t, *J* = 3.0 Hz, CH(*C*H$_3$)$_2$), 17.8 (t, *J* = 3.9 Hz, CH(*C*H$_3$)$_2$).

^{31}P{^{1}H} NMR(δ [ppm], CD_3CN, 20 °C): 131.9.

5.5.2 Preparation of Mo(PNP-^{t}Bu)(CO)$_3$ (6b)

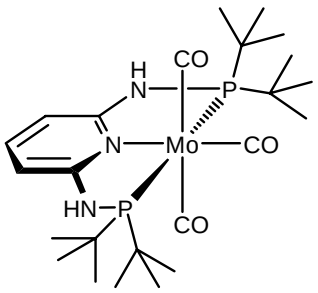

0.284 g	(1.076 mmol)	molybdenumhexacarbonyl
0.429 g	(1.079 mmol)	*N*,*N*'-bis(di-*tert*-butylphosphino)-2,6-diaminopyridine (**5b**)
12 mL		abs. acetonitrile

A Schlenk-flask was loaded with molybdenumhexacarbonyl and 10 mL of abs. acetonitrile were added. The mixture was heated to 85 °C for 5 h. The bright yellow solution was cooled to room temperature and *N*,*N*'-bis(di-*tert*-butylphosphino)-2,6-diaminopyridine (**5b**) and further 2 mL of abs. acetonitrile were added. The solution was stirred at room temperature for 18 h. The solvent was evaporated under vacuum and the crude product purified via column chromatography (neutral Al_2O_3, eluent: methylene chloride).

Yield:	0.092 g (15 %)	brown solid
$C_{24}H_{41}MoN_3O_3P_2$		FW = 577.49 g·mol^{-1}

^{1}H NMR(δ [ppm], CD_2Cl_2, 20 °C): 7.18 (t, *J* = 7.9 Hz, 1H, py^{4}), 6.13 (d, *J* = 8.9 Hz, 2H, py^{3,5}), 5.25 (bs, 2H, N*H*), 1.42-1.35 (m, 36H, C(C*H*$_3$)$_3$).

^{13}C{^{1}H} NMR(δ [ppm], $CDCl_3$, 20 °C): 223.1 (t, *J* = 9.6 Hz, *C*O), 207.3 (t, *J* = 8.4 Hz, *C*O), 160.6 (t, *J* = 6.5 Hz, py^{2,6}), 137.9 (py^{4}), 97.8 (py^{3,5}), 39.9 (t, *J* = 5.0 Hz, *C*(CH$_3$)$_3$), 29.3 (d, *J* = 3.8 Hz, CH(*C*H$_3$)$_2$), 29.2 (d, *J* = 3.8 Hz, C (*C*H$_3$)$_3$).

^{31}P{^{1}H} NMR(δ [ppm], $CDCl_3$, 20 °C): 148.8.

5.5.3 Preparation of W(PNP-^{i}Pr)(CO)$_3$ (6a')

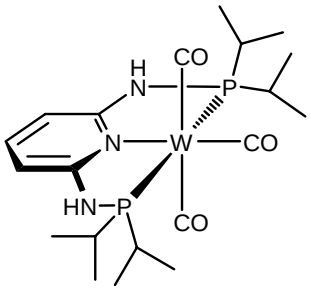

0.555 g	(1.577 mmol)	tungstenhexacarbonyl
0.543 g	(1.590 mmol)	*N,N'*-bis(diisopropylphosphino)-2,6-diaminopyridine (**5a**)
20 mL		abs. acetonitrile

A Schlenk-flask was loaded with tungstenhexacarbonyl and 10 mL of abs. acetonitrile were added. The mixture was heated to 85 °C for 24 h. After cooling to room temperature *N,N'*-bis(diisopropylphosphino)-2,6-diaminopyridine (**5a**) and 5 mL of abs. acetonitrile were added to the bright yellow solution. The reaction mixture was stirred at 80 °C for 20 d. During this period the flask was purged with argon several times to remove carbon monoxide. After cooling to room temperature the solvent was evaporated under vacuum and the raw product purified via column chromatography. The chromatography was performed in two steps. In the first step the product was separated from most of the byproducts (neutral Al_2O_3, eluent: methylene chloride). In the second step the obtained fraction was separated from the remaining free ligand via a second column (neutral Al_2O_3). Therefore the free ligand was eluted with diethyl ether and then the product was eluted with methylene chloride.

Yield:	0.057 g (6 %)	yellow solid
$C_{20}H_{33}WN_3O_3P_2$		FW = 509.30 g·mol^{-1}

^{1}H NMR(δ [ppm], $CDCl_3$, 20 °C): 7.10 (t, *J* = 7.9 Hz, 1H, py^{4}), 6.09 (d, *J* = 7.9 Hz, 2H, py^{3,5}), 5.39 (bs, 2H, N*H*), 2.50-2.21 (m, 4H, C*H*(CH$_3$)$_2$), 1.47-1.06 (m, 24H, CH(C*H*$_3$)$_2$).

^{13}C{^{1}H} NMR(δ [ppm], $CDCl_3$, 20 °C): 234.7 (*C*O), 209.4 (*C*O), 161.6 (py^{2,6}), 137.0 (py^{4}), 96.8 (py^{3,5}), 32.6 (t, *J* = 12.1 Hz, *C*H(CH$_3$)$_2$), 18.9 (CH(*C*H$_3$)$_2$), 18.5 (CH(*C*H$_3$)$_2$).

^{31}P{^{1}H} NMR(δ [ppm], $CDCl_3$, 20 °C): 117.8.

5.5.4 Preparation of Mo(PN(P)-^{i}Pr)(CO)$_4$ (7a)

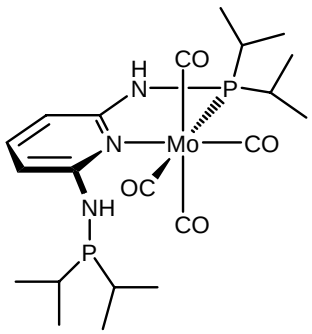

1.049 g	(3.973 mmol)	molybdenumhexacarbonyl
1.357 g	(3.975 mmol)	*N*,*N*'-Bis(diisopropylphosphino)-2,6-diaminopyridine (**5a**)
25 mL		abs. acetonitrile

A 100 mL three-necked round-bottom flask equipped with a reflux-condenser, a septum and a connection to the Schlenk line was loaded with molybdenumhexacarbonyl and 25 mL of abs. acetonitrile were added. The mixture was stirred at 70 °C for 3 h. During the heating the solution was purged with argon several times. The bright yellow solution was cooled to room temperature and *N*,*N*'-bis(diisopropylphosphino)-2,6-diaminopyridine (**5a**) dissolved in 4 mL of abs. acetonitrile was added via a syringe through the septum. The solution was stirred at room temperature for 18 h. Then the reflux-condenser and the septum were replaced by plugs and the solvent was evaporated. The crude product was purified via column chromatography (neutral Al_2O_3, eluent: methylene chloride).

Yield:	1.194 g (58 %)	brown solid
$C_{21}H_{33}MoN_3O_4P_2$		FW = 549.40 g·mol^{-1}

^{1}H NMR(δ [ppm], $CDCl_3$, 20 °C): 7.19 (t, *J* = 8.0 Hz, 1H, py^{4}), 6.76 (dd, *J* = 8.0 Hz, *J* = 3.7 Hz, 1H, py^{3,5}), 6.22 (d, *J* = 10.1 Hz, 1H, N*H*PR$_2$-Mo), 6.07-5.98 (m, 1H, py^{3,5}), 5.18 (bs, 1H, N*H*PR$_2$), 2.43-2.22 (m, 2H, C*H*(CH$_3$)$_2$), 2.13-2.03 (m, 2H, C*H*(CH$_3$)$_2$), 1.50-1.30 (m, 24H, CH(C*H*$_3$)$_2$).

^{13}C{^{1}H} NMR(δ [ppm], $CDCl_3$, 20 °C): 219.0 (6, *J* = 8.8 Hz, *C*O), 213.2 (d, *J* = 10.2 Hz, *C*O), 206.2 (d, *J* = 9.2 Hz, *C*O), 158.4-157.7 (m, py^{2,6}), 135.0 (py^{4}), 97.0 (d, *J* = 25.4 Hz, py^{3,5}), 95.8 (d, *J* = 5.3 Hz, py^{3,5}), 29.7 (t, *J* = 9.5 Hz, *C*H(CH$_3$)$_2$), 28.1 (t, *J* = 19.7 Hz, *C*H(CH$_3$)$_2$), 23.7 (d, *J* = 11.0 Hz, *C*H(CH$_3$)$_2$), 16.8-15.4 (m, CH(*C*H$_3$)$_3$).

^{31}P{^{1}H} NMR(δ [ppm], $CDCl_3$, 20 °C): 110.7 (s, NH*P*R$_2$-Mo), 56.7 (s, NH*P*R$_2$).

5.5.5 Preparation of Mo(PN(P)-^{t}Bu)(CO)$_4$ (7b)

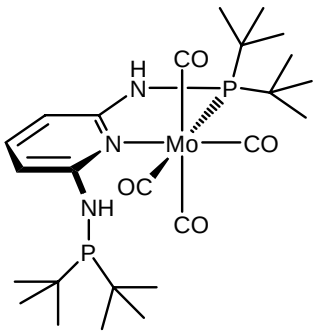

0.280 g	(1.061 mmol)	molybdenumhexacarbonyl
0.421 g	(1.059 mmol)	*N*,*N*'-bis(di-*tert*-butylphosphino)-2,6-diaminopyridine (**5b**)
10 mL		abs. acetonitrile

A Schlenk-flask was loaded with molybdenumhexacarbonyl and 10 mL of abs. acetonitrile were added. The mixture stirred at 70 °C for 3 h. The bright yellow solution was cooled to room temperature and *N*,*N*'-bis(di-*tert*-butylphosphino)-2,6-diaminopyridine was added. The solution was stirred at room temperature for 18 h. The solvent was evaporated under vacuum and the raw product purified via column chromatography (neutral Al_2O_3, eluent: methylene chloride).

Yield:	0.173 g (27 %)	brown solid
$C_{25}H_{41}MoN_3O_4P_2$		FW = 605.50 g·mol^{-1}

^{1}H NMR(δ [ppm], d_6-acetone, 20 °C): 7.34 (t, *J* = 7.9 Hz, 1H, py^4), 7.01-6.86 (m, 2H, py^{3,5}, N*H*PR$_2$-Mo), 6.41 (d, *J* = 7.9 Hz, 1H, py^{3,5}), 6.18 (d, *J* = 10.7 Hz, 1H, N*H*PR$_2$), 1.41 (d, *J* = 13.7 Hz, 18H, C(C*H*$_3$)$_3$), 1.26 (d, *J* = 12.2 Hz, 18H, C(C*H*$_3$)$_3$).

^{13}C{^{1}H} NMR(δ [ppm], d_6-acetone, 20 °C): 210.7 (d, *J* = 8.6 Hz, *C*O), 205.2 (*C*O), 159.5 (py^{2,6}), 137.9 (py^4), 105.5 (d, *J* = 29.9 Hz, py^{3,5}), 99.7 (d, *J* = 5.2 Hz, py^{3,5}), 38.2 (d, *J* = 10.3 Hz, *C*(CH$_3$)$_3$), 34.1 (d, *J* = 21.3 Hz, *C*(CH$_3$)$_3$), 28.4 (C(*C*H$_3$)$_3$), 28.3 (C(*C*H$_3$)$_3$), 28.1 (C(*C*H$_3$)$_3$), 27.9 (C(*C*H$_3$)$_3$).

^{31}P{^{1}H} NMR(δ [ppm], d_6-acetone, 20 °C): 126.2 (s, NH*P*R$_2$-Mo), 71.5 (s, NH*P*R$_2$)

5.6 Reactions of the Complexes

5.6.1 Reaction with Halogens

1. Preparation of [Mo(PNP-^{i}Pr)(CO)$_3$I]I (8a)

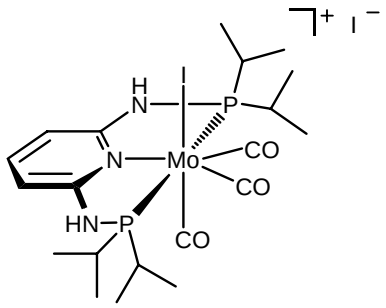

i) Preparation from Mo(PNP-^{i}Pr)(CO)$_3$ (6a) and Iodine as starting materials

0.151 g	(0.290 mmol)	Mo(PNP-^{i}Pr)(CO)$_3$ (**6a**)
0.075 g	(0.295 mmol)	iodine
10 mL		abs. methylene chloride

A Schlenk-flask was loaded with Mo(PNP-^{i}Pr)(CO)$_3$ (**6a**) and 10 mL of abs. methylene chloride were added. Iodine was added, whereupon the color of the mixture changed to dark red. The mixture was stirred for 1 h at room temperature and afterwards the solvent was evaporated. The product was dried under high vacuum without further purification.

Yield:	0.217 g (97 %)	dark-red solid

ii) Preparation from MoI$_2$(CO)$_3$(NCCH$_3$)$_2$ (2) and PNP-^{i}Pr (5a) as starting materials

0.084 g	(0.246 mmol)	PNP-^{i}Pr (**5a**)
0.128 g	(0.248 mmol)	MoI$_2$(CO)$_3$(NCCH$_3$)$_2$ (2)
1 mL		d$_2$-methylene chloride

A NMR-tube was loaded with PNP-^{i}Pr (**5a**) and put under inert atmosphere (argon). The solid was dissolved in 1 mL of d_2-methylene chloride and $MoI_2(CO)_3(NCCH_3)_2$ (**2**) was added. The reaction was monitored via $^{31}P\{^{1}H\}$ NMR spectroscopy and after 30 min. complete conversion was observed.

Yield: Product not isolated

$C_{20}H_{33}I_2MoN_3O_3P_2$ FW = 775.20 g·mol^{-1}

^{1}H NMR(δ [ppm], CD_2Cl_2, 20 °C): 8.10 (bs, 2H, N*H*), 7.41 (bs, 1H, py^{4}), 7.21-7.03 (m, 2H, py^{3,5}), 3.87-3.65 (m, 2H, C*H*$(CH_3)_2$), 3.14-2.84 (m, 2H, C*H*$(CH_3)_2$), 1.70-1.16 (m, 24H, CH(C*H*$_3)_2$).

$^{31}P\{^{1}H\}$ NMR(δ [ppm], CD_2Cl_2, 20 °C): 114.0.

2. Preparation of [Mo(PNP-^{i}Pr)(CO)$_3$Br]Br (9a)

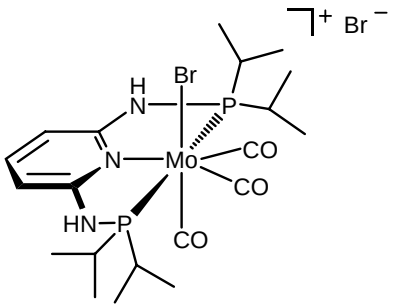

0.170 g	(0.326 mmol)	Mo(PNP-^{i}Pr)(CO)$_3$ (**6a**)
0.055 g	(0.344 mmol)	bromine
10 mL		abs. methylene chloride

A Schlenk-flask was loaded with Mo(PNP-^{i}Pr)(CO)$_3$ (**6a**) and 10 mL of abs. methylene chloride were added. The mixture was cooled to 0 °C and bromine was added, whereupon the color of the mixture changed to dark red. The mixture was warmed to room temperature and after 24 h of stirring the solvent was evaporated. The crude product was washed two times with 5 mL n-pentane and dried under high vacuum.

Yield: 0.209 g (94 %) red-brown solid

$C_{20}H_{33}Br_2MoN_3O_3P_2$ FW = 681.20 g·mol^{-1}

^{1}H NMR(δ [ppm], CD_2Cl_2, 20 °C): 8.73 (bs, 1H, N*H*), 8.30 (bs, 1H, N*H*), 7.42-7.31 (m, 1H, py^{4}), 7.09 (d, *J* = 7.9 Hz, 1H, py^{3,5}), 6.73 (d, *J* = 7.9 Hz, 1H, py^{3,5}), 3.58-3.35 (m, 1H, C*H*$(CH_3)_2$), 2.87-2.61 (m, 3H, C*H*$(CH_3)_2$), 1.62-1.10 (m, 24H, CH(C*H*$_3)_2$).

^{31}P{^{1}H} NMR(δ [ppm], CD_2Cl_2, 20 °C): 117.0.

3. Preparation of [Mo(PNP-^{i}Pr)(CO)$_3$I](SbF$_6$) (8a')

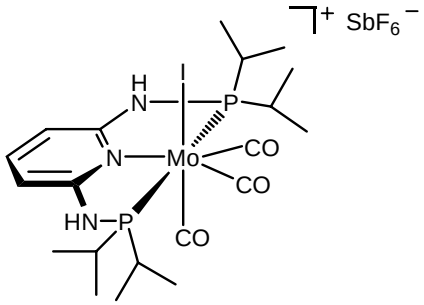

0.152 g	(0.292 mmol)	Mo(PNP-^{i}Pr)(CO)$_3$ (**6a**)
0.077 g	(0.303 mmol)	iodine
0.106 g	(0.308 mmol)	$AgSbF_6$
7 mL		abs. methylene chloride

A Schlenk-flask was loaded with Mo(PNP-^{i}Pr)(CO)$_3$ (**6a**) and 7 mL of abs. methylene chloride were added. The mixture was cooled to 0 °C and iodine was added, whereupon the color of the mixture changed to dark red. The mixture was stirred for 3 h at room temperature and $AgSbF_6$ was added. After 2 h of stirring at room temperature, the precipitated AgI was filtered off through a syringe filter (0.2 µm PTFE). The solvent was evaporated and the product dried under vacuum.

Yield:	0.251 g (97 %)	dark-red solid
$C_{20}H_{33}F_6IMoN_3O_3P_2Sb$		FW = 884.03 g·mol^{-1}

^{1}H NMR(δ [ppm], CD_2Cl_2, 20 °C): 7.55 (bs, 1H, py^{4}), 6.74-6.52 (m, 2H, py^{3,5}), 6.29 (bs, 2H, N*H*), 3.92-3.68 (m, 2H, C*H*$(CH_3)_2$), 2.98-2.70 (m, 2H, C*H*$(CH_3)_2$), 1.74-1.12 (m, 24H, CH(C*H*$_3)_2$)

^{31}P{^{1}H} NMR(δ [ppm], CD_2Cl_2, 20 °C): 112.8.

4. Preparation of [Mo(PNP-^{i}Pr)(CO)$_2$(NCCH$_3$)I]I (8b)

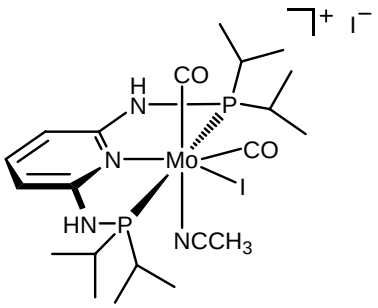

0.302 g	(0.579 mmol)	Mo(PNP-^{i}Pr)(CO)$_3$ (**6a**)
0.147 g	(0.579 mmol)	iodine
10 mL		abs. acetonitrile

A Schlenk-flask was loaded with Mo(PNP-^{i}Pr)(CO)$_3$ (**6a**) and 10 mL of abs. acetonitrile were added. Iodine was added, whereupon the color of the mixture changed to dark red and a yellow solid precipitated. The mixture was stirred for 18 h at room temperature whereupon the color of the precipitate changed to dark red. The solvent was evaporated and the product was dried under high vacuum.

Yield:	0.449 (98 %)	dark-red solid
$C_{21}H_{36}I_2MoN_4O_2P_2$		FW = 788.24 g·mol^{-1}

^{1}H NMR(δ [ppm], CD_3CN, 20 °C): 7.98 (bs, 1H, N*H*), 7.62-7.43 (m, 2H, N*H*, py[4]), 7.01 (d, *J* = 8.1 Hz, 1H, py[3,5]), 6.88 (d, *J* = 8.1 Hz, 1H, py[3,5]), 3.74-3.55 (m, 1H, C*H*(CH$_3$)$_2$), 3.05-2.84 (m, 3H, C*H*(CH$_3$)$_2$), not observed (s, 3H, NCC*H*$_3$), 1.63-1.11 (m, 24H, CH(C*H*$_3$)$_2$).

^{31}P{^{1}H} NMR(δ [ppm], CD_3CN, 20 °C): 113.8.

5.6.2 Preparation of Mo(PNP-^{i}Pr)(CO)$_2$(NCCH$_3$) (11)

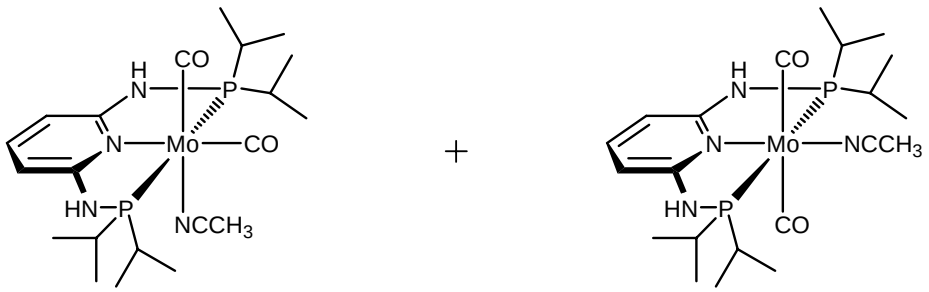

0.070 g	(0.089 mmol)	[Mo(PNP-^{i}Pr)(CO)$_2$(NCCH3)I]I (**8b**)
0.012 g	(0.184 mmol)	Zn
1 mL		d_3-acetonitrile

A NMR tube was loaded with [Mo(PNP-^{i}Pr)(CO)$_2$(NCCH3)I]I (**8b**) and put under inert atmosphere (argon). The solid was dissolved in 1 mL of d_3-acetonitrile and Zn was added. The color of the solution changed from dark red to orange. After 1 h at room temperature the reaction was monitored via ^{1}H and ^{31}P{^{1}H} NMR spectroscopy. Complete conversion was determined. The product was not isolated.

Yield:	product not isolated
$C_{21}H_{36}MoN_4O_2P_2$	FW = 534.43 g·mol^{-1}

^{1}H NMR(δ [ppm], CD_3CN, 20 °C): 7.45 (t, *J* = 7.6 Hz, 1H, py^{4}), 6.86 (s, 2H, N*H*), 6.44 (d, *J* = 7.6 Hz, 2H, py^{3,5}), 2.79-2.61 (m, 2H, C*H*(CH$_3$)$_2$), 2.57-2.40 (m, 2H, C*H*(CH$_3$)$_2$), 2.17 (3H, NCCH$_3$), 1.51-1.03 (m, 24H, CH(C*H*$_3$)$_2$).

^{31}P{^{1}H} NMR(δ [ppm], CD_3CN, 20 °C): 123.4, 123.1.

5.6.3 Reaction of Mo(PNP-^{i}Pr)(CO)$_3$ (6a) with CF_3COOH

0.067 g	(0.129 mmol)	Mo(PNP-^{i}Pr)(CO)$_3$ (**6a**)
0.015 g	(0.132 mmol)	trifluoroacetic acid
1 mL		d_3-acetonitrile

A NMR tube was loaded with Mo(PNP-^{i}Pr)(CO)$_3$ (**6a**) and put under inert atmosphere (argon). The solid was dissolved in 1 mL of d_3-acetonitrile and trifluoroacetic acid was added. After 1 h at room temperature the reaction was monitored via ^{1}H and ^{31}P{^{1}H} NMR spectroscopy. The product was not isolated.

Yield: product not isolated

^{1}H NMR(δ [ppm], CD_3CN, 20 °C): 7.42 (t, *J* = 8.0 Hz, 1H, py^{4}), 6.93 (d, 2H, N*H*), 6.38 (d, *J* = 8.0 Hz, 2H, py^{3,5}), 2.78-2.52 (m, 4H, C*H*(CH_3)$_2$), 1.47-1.11 (m, 24H, CH(C*H*$_3$)$_2$), -5.32, -5.46, -5.61.

^{31}P{^{1}H} NMR(δ [ppm], CD_3CN, 20 °C): not observed.

5.6.4 Self-Exchange Atom Transfer Experiment

0.017 g	(0.019 mmol)	Mo(PNP-^{i}Pr)(CO)$_3$ (**6a**)
0.010 g	(0.019 mmol)	[Mo(PNP-^{i}Pr)(CO)$_3$I](SbF$_6$) (**8a'**)
1 mL		d_2-methylene chloride

A NMR tube was loaded with Mo(PNP-^{i}Pr)(CO)$_3$ (**6a**) and [Mo(PNP-^{i}Pr)(CO)$_3$I](SbF$_6$) (**8a'**) and put under inert atmosphere (argon). 1 mL of d_2-methylene chloride was added and the complexes dissolved. The reaction mixture was monitored via ^{31}P{^{1}H} NMR spectroscopy after 1 h. The reaction mixture was warmed to 50 °C and after 1 h again monitored via ^{31}P{^{1}H} NMR spectroscopy.

5.7 Crystallographic data

Table 5.1 Crystal data and structure refinement for [Mo(PNP-^{i}Pr)(CO)$_3$Br]Br

Empirical formula	$C_{20}H_{33}Br_2MoN_3O_3P_2$
Formula weight	681.19
Temperature	173(2) K
Wavelength	0.71073 Å
Crystal system, space group	Monoclinic, C2/c
Unit cell dimensions	a = 29.6913(15) Å α = 90° b = 10.7919(5) Å β = 97.954(1)° c = 16.7764(8) Å γ = 90°
Volume	5323.9(4) Å^3
Z	8
Calculated density	1.700 Mg·m^3
Absorption coefficient	3.640 mm^{-1}
F(000)	2720
Crystal size	0.33 x 0.30 x 0.19 mm, yellow plate
Diffractometer	Bruker SMART APEX CCD 3-circle (sealed X-ray tube, Mo K_α rad., graphite monochromator, detector distance 50 mm, 512x512 pixels)
Scan type / width / speed	ω-scan frames / dome=0.3° / 20s/frame full sphere data collection, 4 x 606 frames
Theta range for data collection	2.30 to 30.00°
Index ranges	$-41 \le h \le 41$, $-15 \le k \le 15$, $-23 \le l \le 23$
Reflections collected / unique	36362 / 7732 [R(int) = 0.0224]
Completeness to theta = 30.00	99.5%
Absorption correction	Multi-scan (program SADABS; Sheldrick, 1996)
Max. and min. transmission	0.50 and 0.32
Structure solution	Direct methods (program SHELXS97)
Refinement method	Full-matrix least-squares on F2 (program SHELXL97)
Data / restraints / parameters	7732 / 96 / 294
Goodness-of-fit on F^2	1.028
Final R indices [I > 2σ(I)]	R_1 = 0.0273, ωR_2 = 0.0693 (6562 data)
R indices (all data)	R_1 = 0.0351, ωR_2 = 0.0734 (7732 data)
Largest diff. peak and hole	0.97 and -1.01 eA^{-3}

$$R_1 = \frac{\sum \left| |F_0| - |F_c| \right|}{\sum |F_0|} \qquad \omega R_2 = \left[\frac{\sum \omega \left(F_0^2 - F_c^2 \right)^2}{\sum \omega \left(F_0^2 \right)^2} \right]^{\frac{1}{2}}$$

Table 5.2 Bond lengths for [Mo(PNP-^{i}Pr)(CO)$_3$Br]Br

bond	bond length [Å]	bond	bond length [Å]
Mo-C(19)	1.979(2)	C(7)-H(7A)	0.98
Mo-C(20)	2.006(2)	C(7)-H(7B)	0.98
Mo-C(18)	2.037(2)	C(7)-H(7C)	0.98
Mo-N(1)	2.2364(15)	C(8)-H(8A)	0.98
Mo-P(2)	2.5172(5)	C(8)-H(8B)	0.98
Mo-P(1)	2.5242(5)	C(8)-H(8C)	0.98
Mo-Br(1)	2.6713(3)	C(9)-C(11)	1.524(4)
P(1)-N(2)	1.6856(17)	C(9)-C(10)	1.540(3)
P(1)-C(6)	1.838(2)	C(9)-H(9)	1.00
P(1)-C(9)	1.858(2)	C(10)-H(10A)	0.98
P(2)-N(3)	1.6812(17)	C(10)-H(10B)	0.98
P(2)-C(15)	1.840(2)	C(10)-H(10C)	0.98
P(2)-C(12)	1.852(2)	C(11)-H(11A)	0.98
O(1)-C(18)	1.076(3)	C(11)-H(11B)	0.98
O(2)-C(19)	1.140(3)	C(11)-H(11C)	0.98
O(3)-C(20)	1.125(3)	C(12)-C(14)	1.527(4)
N(1)-C(1)	1.365(2)	C(12)-C(13)	1.529(3)
N(1)-C(5)	1.366(2)	C(12)-H(12)	1.00
N(2)-C(1)	1.383(3)	C(13)-H(13A)	0.98
N(2)-H(2N)	0.88000(12)	C(13)-H(13B)	0.98
N(3)-C(5)	1.376(2)	C(13)-H(13C)	0.98
N(3)-H(3N)	0.88000(16)	C(14)-H(14A)	0.98
C(1)-C(2)	1.393(3)	C(14)-H(14B)	0.98
C(2)-C(3)	1.383(3)	C(14)-H(14C)	0.98
C(2)-H(2)	0.95	C(15)-C(17)	1.526(3)
C(3)-C(4)	1.380(3)	C(15)-C(16)	1.529(3)
C(3)-H(3)	0.95	C(15)-H(15)	1.00
C(4)-C(5)	1.385(3)	C(16)-H(16A)	0.98
C(4)-H(4)	0.95	C(16)-H(16B)	0.98
C(6)-C(8)	1.518(4)	C(16)-H(16C)	0.98
C(6)-C(7)	1.534(3)	C(17)-H(17A)	0.98
C(6)-H(6)	1.00	C(17)-H(17B)	0.98
		C(17)-H(17C)	0.98

Table 5.3 Hydrogen bonds in Mo(PNP-^{i}Pr)(CO)$_3$

D–H···A	**d(D–H)**	**d(H···A)**	**d(D···A)**	**<(DHA)**
N(2)–H(2N)···Br(2)	0.88	2.406(6)	3.2674(16)	166(2)
N(3)–H(3N)···Br(2)#1	0.88	2.430(3)	3.3053(17)	173(2)

Symmetry transformations used to generate equivalent atoms #1: $x, -y, z-\frac{1}{2}$

Bibliography

[1] van Koten, G.; Timer; K., Noltes, J. G.; Spek, A. L. *J. Chem. Soc. Chem. Commun.* **1978**, 250.

[2] Moulton, C. J.; Shaw, B. L. *J. C. S. Dalton* **1976**, 1020.

[3] Singleton, J T. *Tetrahedron* **2003**, *59*, 1837.

[4] (a) Schirmer, W.; Flörke, U.; Haupt, H.-J. *Z. anorg. Allg. Chem.*, **1987**, *545*, 83. (b) Schirmer, W.; Flörke, U.; Haupt, H.-J. *Z. anorg. Allg. Chem.*, **1989**, *574*, 239.

[5] Benito-Garagorri, D.; Becker, E.; Wiedermann, J.; Lackner, W.; Pollak, M.; Mereiter, K.; Kisala, J.; Kirchner, K. *Organometallics* **2006**, *25*, 1900.

[6] Benito-Garagorri, D.; Bocokić, V.; Mereiter K.; Kirchner, K. *Organometallics*, **2006**, *25*, 3817.

[7] Lang, H.-F.; Fanwick, P. E.; Walton, R. A. *Inorg. Chim. Acta* **2002**, *329*, 1.

[8] (a) Doney, J. J.; Bergman, R. J.; Heathcock, C. H. *J. Am. Chem. Soc.* **1985**, *107*, 3724. (b) Hughes, R. P.; Klaeui, W.; Reisch, J. W.; Mueller, A. *Organometallics* **1985**, *4*, 1761.

[9] (a) Trofimenko, S. *J. Am. Chem. Soc.* **1967**, *89*, 3904. (b) Trofimenko, S. *J. Am. Chem. Soc.*, **1969**, *91*, 588. (c) Enemark, J. H.; Marabella, P. *J. Organomet. Chem.* **1982**, *226*, 57. (d) Shiu, K.-B.; Lee, J. Y.; Wang, Y.; Cheng, M.-C.; Wang, S.-L.; Liao, F.-L. *J. Organomet. Chem.* **1993**, *453*, 211.

[10] (a) Castonguay, A.; Sui-Seng, C.; Zaragarina, D.; Beauchamp, A. L. *Organometallics* **2006**, *25*, 602. (b) Danopoulos, A. A.; Tulloch, A. A. D.; Winston, S.; Eastham, G.; Hursthouse, M. B. *Dalton Trans.* **2003**, 1009. (c) Churruca, F.; SanMartin, R.; Tellitu, I.; Domínguez, E. *Tetrahedron Lett.*, **2006**, *47*, 3233.

[11] (a) Peveling, K.; Henn, M.; Loew, C.; Mehring, M.; Schuermann, M.; Costisella, B.; Jurkschat, K. **2004**, *23*, 1501. (b) Yao, Q.; Sheets, M. *J. Org. Chem.* **2006**, *71*, 5384. (c) van Manen, H.-J.; Nakashima, K.; Shinkai, S.; Kooijman, H.; Spek, A. L.; van Veggel, F. C. J. M.; Reinhoudt, D. N. *Eur. J. Inorg. Chem.* **2000**, 2533.

[12] Poverenov, E.; Gandelman, M.; Shimon, L. J. W.; Rozenberg, H.; Ben-David, Y.; Milstein, D. *Chem. Eur. J.* **2004**, *10*, 4673.

[13] Albrecht, M.; van Koten, G. *Angew. Chem. Int. Ed.* **2001**, *40*, 3750.

[14] Steenwinkel, P.; Gossage, R. A.; van Koten, G. *Chem. Eur. J.*, **1998**, *4*, 759.

[15] Myazaki, F.; Yamaguchi, K.; Shibasaki, M. *Tetrahedron Lett.*, **1999**, *40*, 7379.

[16] Van de Kuil, L. A.; Luitjes, H.; Grove, D. M.; Zwikker, J. W.; van den Linden, J. G. M.; Roelofsen, A. M.; Jenneskens, L. W.; Drenth, W.; van Koten, G. *Organometallics*, **1994**, *13*, 468.

[17] (a) Dahlhoff, W. V.; Nelson, s. M. *J. Chem. Soc. A* **1971**, 2184. (b) Hahn, C.; Spiegler, M.; Herdtweck, E.; Taube, R. *Eur. J. Inorg. Chem.* **1999**, 435. (c) Abbenhuis, R. A. T. M.; del Rio, I.; Bergshoef, M. M.; Boersma, J.; Veldman, M.; Spek, A. L.; van Koten, G. *Inorg. Chem.* **1998**, *37*, 1749. (d) Zhang, J.; Leitus, G.; Ben-David, Y.; Milstein, D. *J. Am. Chem. Soc.* **2005**, *127*, 10840.

[18] Heck, R. F. *J. Am. Chem. Soc.* **1968**, *90*, 5518.

[19] Takenaka, K.; Minakawa, M.; Uozumi, Y. *J. Am. Chem. Soc.* **2005**, *127*, 12273.

[20] Miyaura, M.; Suzuki, A. *Chem. Rev.* **1995**, *95*, 2457.

[21] Guillena, G.; Kruithof, C. A.; Casado, M. A.; Egmond, M. R.; van Koten, G. *J. Organomet. Chem.* **2003**, *668*, 3.

[22] Schrock, R. R. *Topics in Organometallic Chemistry* **1998**, 1, 1.

[23] Indictor, N.; Brill, W. F. *J. Org. Chem.*, **1965**, *30*, 2074.

[24] Mimoun, H.; Serée de Roch, I.; Sajus, L. *Bull. Soc. Chim.*, **1969**, 1481.

[25] Thiel, W. R. *J. Mol. Cat. A* **1997**, *117*, 449.

[26] Kuehn, F. E.; Zhao, J.; Herrmann, W. A. *Tetrahedron: Asymmetry* **2005**, *16*, 3469.

[27] Schrock, R. R. *Acc. Chem. Res.* **2005**, *38*, 955.

[28] Melník, M.; Sharrock, P. *Coord. Chem. Rev.*, **1985**, *65*, 49.

[29] Drew, M. G. B. *Prog. Inorg. Chem.*, **1977**, *23*, 67

[30] Baker, P. K. *Chem. Soc. Rev.*, **1998**, *27*, 125.

[31] (a) Tsarev, V. N.; Kabro, A. A.; Moieseev, S. K.; Kalinin, V. N.; Bondarev, O. G.; Davankov, V. A.; Gavrilov, K. N. *Russ. Chem. Bull., Int. Ed.* **2004**, *53*, 814. (b) van Rooy, A.; Kamer, P. C. J.; van Leeuwen, P. W. N. M.; Goubitz, K.; Fraanje, J.; Veldman, N.; Spek, A. *Organometallics* **1996**, *15*, 835.

[32] Kadyrov, R.; Heller, D.; Selke, R. *Tetrahedron: Asymmetry* **1998**, *9*, 329.

[33] Morales-Morales, D.; Redón, R.; Yung, C.; Jensen, C. M. *Inorg. Chim. Acta*, **2004**, *357*, 2953.

[34] Goettker-Schnetmann, I.; White, P.; Brookhart, M. *J. Am. Chem. Soc.* **2004**, *126*, 1804.

[35] Bocokić, V. *Diploma Thesis*, TU Wien **2006**.

[36] Pollak, M. *Diploma Thesis*, TU Wien **2006**.

[37] Samuel, G. O.; Yankowsky, A. W.; Salvatore, B. A.; Bailey, W. J.; Davidoff, E. F.; Marks, T. J. *Journal of Chemical and Engineering Data* **1970**, *15*, 497.

[38] Tate, D. P.; Knipple, W. R.; Augl, J. M. *Inorg. Chem.* **1962**, *1*, 433.

[39] Stolz, I. W.; Dobson, G. R.; Sheline, R. K. *Inorg. Chem.* **1963**, *2*, 323.

[40] Balakrishna, M. S.; Krishnamurthy, S. S.; Manohar, H. *Organometallics* **1991**, *10*, 2522.

[41] Cano, M.; Campo, J. A.; Heras, J. V.; Pinilla, E.; Monge, A. *Polyhedron* **1996**, *15*, 1705.

[42] Baker, P. K.; Meehan, M. M.; Kwen, H.; Abbott, A. *Inorg. Synth.* **2002**, *33*, 239.

[43] Tom Dieck, H.; Friedel, H.; *J. Organomet. Chem.* **1968**, *14*, 375.

[44] Trofimenko, S. *J. Am. Chem. Soc.* **1969**, *91*, 588.

[45] Schwarz, C. L.; Bullock, R. M.; Creutz, C. *J. Am. Chem. Soc.*, **1991**, *113*, 1225.

[46] (a) Birdwhistell, K. R.; Nieter Burgmayer, S. J.; Templeton, J. L. *J. Am. Chem. Soc.* **1983**, *105*, 7789. (b) Birdwhistell, K. R.; Tonker, T. L.; Templeton, J. L. *J. Am. Chem. Soc.* **1985**, *107*, 4474. (c) Birdwhistell, K. R.; Tonker, T. L.; Templeton, J. L. *J. Am. Chem. Soc.* **1987**, *109*, 1401.

[47] Dilworth, J. R.; Richards, R. L.; Chen, G. J.-J.; McDonald, J. W. *Inorg. Synth.* **1990**, *28*, 33.

[48] Perrin, D. D.; Armarego, W. L. F. *Purification of Laboratory Chemicals*, 3rd ed., Pergamon, New York, **1988**.

[49] Bruker programs: *SMART*, version 5.054; *SAINT*, version 6.2.9; *SADABS*, version 2.10; *XPREP*, version 5.1; *SHELXTL*, version 5.1; Bruker AXS Inc.: Madison, WI, **2001**.

[50] Sheldrick, G. M. *SHELX97*: Program System for Crystal Structure Determination; University of Göttingen: Göttingen, Germany, **1997**.

[51] Spek, A. L. *PLATON: A Multipurpose Crystallographic Tool*; University of Utrecht: Utrecht, The Netherlands, **2004**.